

150442

**THE MATHEMATICAL MODELING OF
VIBRATIONS IN MARINE PIPELINE**

**A Thesis Submitted to the
Graduate School of Natural and Applied Sciences of
Dokuz Eylül University
In Partial Fulfillment of the Requirements for
the Degree of Doctor of Philosophy in Marine Science and Technology, Coastal
Engineering Program**

by

B. Gültekin SINIR

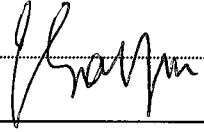
August, 2004

İZMİR

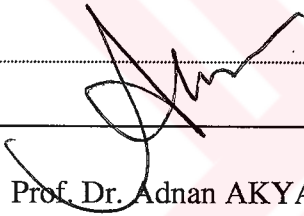
150442

Ph. D. THESIS EXAMINATION RESULT FORM


We certify that we have read this thesis and “THE MATHEMATICAL MODELING OF VIBRATIONS IN MARINE PIPELINE” completed by **B. Gültekin SINIR** under supervision of **Asst. Prof. Dr. Erdem SAYIN** and that in our opinion it is fully adequate, in scope and in quality, as a thesis for the degree of Doctor of Philosophy.



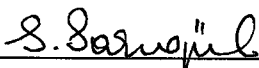
Asst. Prof. Dr. Erdem SAYIN



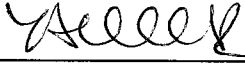
Prof. Dr. Adnan AKYARLI



Assoc. Prof. Dr. Hakan BOYACI

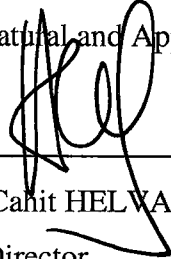


Prof. Dr. A. Saide SARIGÜL



Assoc. Prof. Dr. Ahmet C. YALÇINER

Approved by the
Graduate School of Natural and Applied Sciences



Prof. Dr. Cahit HELVACI

Director

ACKNOWLEDGE

I would like to thank to following who have supported me during this study. First I would like to thank to my advisor Asst. Prof. Dr. Erdem SAYIN for his supervision and encouragement. I have to extend my thanks Prof. Dr. Adnan AKYARLI and Assoc. Prof. Dr. Hakan BOYACI. I would like to acknowledge Assoc. Prof. Dr. Halil Rıdvan ÖZ who provided program and Prof. Dr. Mehmet PAKDEMİRLİ who provided some documents so that I could complete this study. And I would like to thank Bozkurt Burak ÖZHAN.

B. Gültekin SINIR

ABSTRACT

In vibrations of continuous system, types of support conditions are important and have direct effect on the solutions and natural frequencies. In this thesis, the transverse vibrations of pipes conveying fluid with non-ideal boundary conditions are analyzed. Two different types of support conditions are considered: fixed-fixed and clamped-clamped. The flow velocity is assumed to be constant and the pipes are considered as Euler-Bernoulli. The equation of motion is derived using Hamilton's principle and then it is rewritten in non-dimensionalized form. It is solved analytically by direct application of the method of multiple time scales (a perturbation technique). It is also calculated numerically by the finite difference method (FDM). It is found that the types of support conditions have effect on the solutions. Non-ideal boundary conditions alter natural frequencies, stability boundaries and displacements. The non-ideal boundary conditions are assumed that they are moving harmonically with time and their frequencies are equal to natural frequencies of the system. The natural frequencies are found that they are changing with the non-ideal boundary conditions. Increasing amplitudes of displacements or slopes of non-ideal boundary conditions cause a decrease of stable areas of the system. Graphical results in the forms of natural frequencies and stability boundaries are presented for the first and second mode. It is showed that the results obtained by the multiple times scale are agree with the numerical results computed by using FDM. The time histories of displacement calculated by FDM are given for some specific examples.

Keywords: Pipe, vibrations, non-ideal boundary conditions, marine pipeline, finite difference, the method of Multiple Time Scale, perturbations

ÖZET

Sürekli ortamlar titreşimde mesnet tipleri çok önemlidir ve sistemin çözümü ile doğal frekansları üzerinde direk etkisi vardır. Bu tezde akışkan taşıyan boruların enine titreşimi ideal olmıyan sınır şartları altında çözüldü. İki farklı mesnetlenme şekli göz önüne alındı: sabit-sabit ve ankastre-ankastre. Akışkan hızı sabit kabul edildi. Borunun Euler-Bernoulli olduğu düşünöldü. Hareket denklemi Hamilton prensibi kullanılarak çıkarıldı ve boyutsuz formda tekrar yazıldı. Analitik olarak çok zaman ölçekli metot (bir perturbasyon tekniğı) ile çözüldü. Ayrıca sonlu farklar metoduyla hesaplandı. Mesnetlenme şeklinin çözüm üzerinde etkisi olduğu bulundu. İdeal olmıyan sınır şartı, doğal frekansı, stabilite sınırlarını değıştirir. İdeal olmıyan sınır şartının zamanla sistemin doğal frekansına eşit frekansla harmonik olarak hareket ettiği kabul edilmiştir. Doğal frekansın, ideal olmıyan sınır şartıyla değıştığı bulunmuştur. Dönme veya yerdeğıştirme seklindeki ideal olmıyan sınır şartı genliğinin artması sistemin stabil alanın küçölmesine yol açar. Birinci ve ikinci modlar için, doğal frekans ve stabil bölgeler grafik formda sunulmuştur. Çok zaman ölçekli metotdan elde edilen sonuçlarla sonlu farklar metoduyla elde edilen sayısal deęerlerin uyduğu gösterilmiştir. Sonlu farklarla hesaplanan zamanla yer değıştirme grafikleri bir kaç sembolik örnek için verilmiştir.

Anahtar kelimeler: Boru, titreşim, ideal olmıyan sınır şartı, deniz boru hatları, sonlu farklar, çok zaman ölçekli metot, perturbasyon.

CONTENTS

Contents.	VII
List of Figures.	IX
List of Tables.	XI
List of Symbols.	XIII

Chapter One INTRODUCTION

1.1. Literature Review.	1
1.2. Marine Pipeline.	4
1.3. Statement of the Problem.	14

Chapter Two THE EQUATION OF MOTION

2.1. The Equation of Motions.....	6
2.2. Non-dimensionalized of the Equation.....	9

Chapter Three SOLUTIONS OF THE EQUATION OF MOTION FOR NON-IDEAL BOUNDARY CONDITIONS

3.1 Introduction.....	10
3.2 Solution for Fixed-Fixed Pipes.....	12
3.2.1 Numerical Results.....	20

3.3 Solution for Clamped-Clamped Pipes.....	26
3.3.1 Numerical Results.....	30

Chapter Four
FINITE DIFFERENCE SOLUTION OF THE EQUATION OF MOTION

4.1 Finite Difference Solution of the Equation of Motion.....	40
4.2 Numerical Results.....	43
Conclusion.....	48
References.....	49



LIST OF FIGURES

Figure 1.1 Sandbagging [Melegari&Bressan (1990)]	7
Figure 1.2 Grouting (support) [Melegari&Bressan (1990)]	8
Figure 1.3 Jack ups (mechanical supports) [Melegari&Bressan (1990)]	10
Figure 1.4 Grouting (protection) [Melegari&Bressan (1990)]	11
Figure 1.5 Bitumen mattress [Melegari&Bressan (1990)]	12
Figure 1.6 Concrete mattress [Melegari&Bressan (1990)]	12
Figure 1.7 Concrete saddle [Melegari&Bressan (1990)]	13
Figure 2.1 Schematics of translating continua in a pipe with fixed-fixed supports ...	17
Figure 2.2 Schematics of translating continua in a pipe with clamped-clamped supports	18
Figure 3.1 Schematics of translating continua in a pipe with fixed-fixed supports ...	24
Figure 3.2 Comparisons of the first natural frequencies for different non-ideal boundary conditions for fixed-fixed supports ($\beta=0.8$, $\epsilon=0.1$, $\mu=1.0$).....	35
Figure 3.3 Comparisons of the second natural frequencies for different non-ideal boundary conditions for fixed-fixed supports ($\beta=0.8$, $\epsilon=0.1$, $\mu=1.0$).....	36
Figure 3.4 Variation of stability boundaries for constant amplitude of right-hand side for the first mode ($\beta=0.8$, $\epsilon=0.1$, $\mu=1.0$).	37
Figure 3.5 Variation of stability boundaries for constant amplitude of right-hand side for the first mode ($\beta=0.8$, $\epsilon=0.1$, $\mu=0.5$).	37

Figure 3.6 Variation of stability boundaries for constant amplitude of right-hand side for the second mode ($\beta=0.8, \epsilon=0.1, \mu=1.0$).....	39
Figure 3.7 Variation of stability boundaries for constant flow velocities for the first mode ($\beta=0.8, \epsilon=0.1, \mu=1.0$).	40
Figure 3.8 Variation of stability boundaries for constant flow velocities for the second mode ($\beta=0.8, \epsilon=0.1, \mu=1.0$).	40
Figure 3.9 Schematics of translating continua in a pipe with clamped-clamped supports	41
Figure 3.10 Comparisons of first natural frequencies for different non-ideal boundary conditions for clamped-clamped supports ($\beta=0.8, \epsilon=0.1, \mu=1.0$)	47
Figure 3.11 Comparisons of second natural frequencies for different non-ideal boundary conditions for clamped-clamped supports ($\beta=0.8, \epsilon=0.1, \mu=1.0$)	48
Figure 3.12 Variation of stability boundaries for constant amplitude of right-hand side for the first mode ($\beta=0.8, \epsilon=0.1, \mu=1.0, a_1=0, b_1=0$).	49
Figure 3.13 Variation of stability boundaries for constant amplitude of right-hand side for the first mode ($\beta=0.8, \epsilon=0.1, \mu=0.5, a_1=0, b_1=0$).	50
Figure 3.14 Variation of stability boundaries for constant amplitude of right-hand side for the first mode ($\beta=0.8, \epsilon=0.1, \mu=1.0, a_1=0.2, b_1=0.2$).	50
Figure 3.15 Variation of stability boundaries for constant amplitude of right-hand side for the first mode ($\beta=0.8, \epsilon=0.1, \mu=1.0, a_1=0.5, b_1=0.5$).	51
Figure 3.16 Variation of stability boundaries for constant amplitude of right-hand side for the second mode ($\beta=0.8, \epsilon=0.1, \mu=1.0, a_1=0.0, b_1=0.0$).	52
Figure 3.17 Variation of stability boundaries for constant amplitude of right-hand side for the second mode ($\beta=0.8, \epsilon=0.1, \mu=1.0, a_1=0.2, b_1=0.2$).	53
Figure 3.18 Variation of stability boundaries for constant amplitude of right-hand side for the second mode ($\beta=0.8, \epsilon=0.1, \mu=1.0, a_1=0.5, b_1=0.5$)	53
Figure 3.19 Variation of stability boundaries for constant flow velocities for the first mode ($\beta=0.8; \epsilon=0.1; () a=0.0, b=0.0; () a=0.2, b=0.2; () a=0.5, b=0.5, \mu=1.0$).	54
Figure 3.20 Variation of stability boundaries for constant flow velocities for the second mode ($\beta=0.8, \epsilon=0.1, \mu=1.0, a_1=0.0, b_1=0.0$)	55

Figure 3.21 Variation of stability boundaries for constant flow velocities for the second mode ($\beta=0.8, \epsilon=0.1, \mu=1.0, a_1=0.2, b_1=0.2$)	56
Figure 3.22 Variation of stability boundaries for constant flow velocities for the second mode ($\beta=0.8, \epsilon=0.1, \mu=1.0, a_1=0.5, b_1=0.5$)	56
Figure 4.1. The displacement histories of fixed-fixed supports for simple beam with ideal conditions.....	61
Figure 4.2. The displacement histories of fixed-fixed supports for simple beam with non-ideal conditions.	62
Figure 4.1. The displacement histories of clamped-clamped supports, for $a_1=b_1=0$..	65
Figure 4.2. The displacement histories of clamped-clamped supports, for $a_1=b_1=0.02$	65
Figure 4.3. The displacement histories of fixed-fixed supports for $b_0=0.0$	66
Figure 4.4. The displacement histories of fixed-fixed supports for $b_0=0.05$	66

LIST OF TABLES

- Table 4.1 The values obtained by using the Multiple Time Scale for clamped-clamped supports ($a_0=b_0=0.1$, $v=5.0$, $c=0.025$, $\theta=0.0$, $\varepsilon=0.1$, $\mu=1.0$).....64
- Table 4.2 The values obtained by using the Multiple Time Scale for fixed-fixed supports ($a_0=0.2$, $v=2.4$, $c=0.04$, $\theta=0.0$, $\varepsilon=0.1$, $\mu=1.0$)64



LIST OF SYMBOLS

y^*	transverse displacement
Y	non-dimensional transverse displacement
v	fluid velocity
V	non-dimensional fluid velocity
ρ_f	fluid density
ρ_p	pipe density
A_p	cross-sectional area of the pipe
A_f	cross-sectional area of the fluid
L	length of the pipe
E_p	module of the elasticity of the pipe
t^*	time
t	non-dimensional time
T	total kinetic energy of the system
T_p	kinetic energy of the pipe
T_f	kinetic energy of the fluid
U	elastic energy of the system
\mathcal{E}	Lagrangian of the system
F	functional of the system
λ	linear viscous damping coefficient
k	linear foundation coefficient
K	non-dimensional linear foundation coefficient
f	force term
F	non-dimensional force term
D, μ	non-dimensional viscous damping coefficient
β	ratio of fluid mass
$Y_n(x)$	mode shape

ω_n	natural frequencies
b, b_0	amplitude of right hand side non-ideal condition
a, a_0	amplitude of left hand side non-ideal condition
c, θ	constants
ε	perturbation parameter
Ω	varied natural frequencies
σ	the value obtained by MTSM
m	total mass



CHAPTER ONE

INTRODUCTION

1.1 Literature Review

The subject of pipes conveying fluid has been studied extensively in the literature due to its technical importance. The dynamic of pipe is important problem in a lot of engineering areas such as wastewater discharges, nuclear power plants etc. Of all the studies, information of the natural frequencies and mode shapes of the system is most important and it is the basis of vibration analyses. Furthermore, the stability of a fluid conveying pipe is of practical importance since the natural frequencies of a pipe generally decrease with increasing fluid velocity.

The flow-induced vibration has been studied widely since it always contains a possibility of severe accidents by the several types of vibrations related to a fluid-structure interaction. A fluid flowing through a pipe can impose pressure on the pipe walls and deflect the pipe. It can be seen easily and understood physically that, with increasing flow velocity, the effective stiffness of the system is diminished; for sufficiently large velocity, some events may occur such as, divergence, buckling and pitchfork bifurcation. The study on the flow-induced vibrations has focused both on design and maintenance. The main aims are (1) to supply proper supports to reduce deflection of a system and (2) to find out the fluid velocities that cause system instability.

The paper presented by Paidoussis and Li (1993) reviews the dynamic of pipes conveying fluid and presents a selective review of the undertaken on it. In their

paper, the dynamics of pipes with supported ends, cantilevered pipes or with unusual boundary conditions; continuously flexible pipes or articulated ones; pipe conveying incompressible or compressible fluid, with steady or unsteady flow velocity; pipes thin enough to be treated as thin shells; linear, nonlinear and chaotic dynamics; these and many more are some of the aspects of the problem considered. An Appendix is provided for those unfamiliar with the modern methods of nonlinear analysis.

The selection of the support locations is closely related to the analysis on the natural frequencies and mode shapes of a system. Once proper points are selected, the occurrence of fatigue-related pipe failures due to vibration can be reduced. While the large deflection of a pipe can be main source of the long-term fatigue failures, the system instabilities directly related to the rapid pipe break in a relatively short time duration. If a piping system reach a critical fluid velocity, pipes broken suddenly and discharge fluid of high pressure. Furthermore, broken parts can cause secondary pipe failure due to pipe whipping. These kinds of failure always have the possibility of damaging staff and relevant piping system. [Kang (2000)]

In a cantilevered fluid-conveying pipe the Coriolis force always acts as a damping mechanism that will be referred to as fluid damping [Langthjem and Sugiyama (1999) and Semercigil et al (1997)]. The reaction force due to the momentum flux out of the free end, acts as a follower load, as in Beck's column [Langthjem and Sugiyama (1999)].

Kang (2000) proposed the effect of rotary inertia of concentrated masses attached on the fluid-conveying pipe. The paper written by Koo and Park (1998) shows that if the dominant frequency contents in the excitation loads are known, a proper design of periodic supports for reducing the vibration in those frequency bands is possible.

Numerous investigators concentrates on the effect of foundations on dynamic behaviors of pipes: Impollonia and Elishakoff (2000); Elishakoff and Impollonia (2001); Doare and Langre (2002); De Langre and Ouvrard (1999)

For nonlinear vibration analysis of pipes conveying fluid and for nonlinear fluid-structure problems, many articles have been reported in the literature: Lin and Tsai (1997)(1997), Lam et al. (2002); Gorman et al. (2000), Jensen (1997)

Dynamic behavior of compressed fluid conveying pipe is also analyzed recently by some authors: Guran and Atanackovic (1998); Gaul and Wenzel (2002).

Wu and Shih (2001) determined the lowest natural frequencies and associated normal mode shapes of non-periodic multispan pipe with external load.

Some authors (Zhu 1995, Price et al. 1998) presented motions of thin shells conveying fluid.

In their paper, Wang And Bloom (1999) formulated a mathematical model to study the dynamic of submerged and inclined concentric pipes with different lengths and identified a few critical parameters pertaining to the proper design of such pipe systems.

Vendhan et al (1997) give very good and simple analytic solution technique conveying fluid flexible cylinder.

A lot of reports on the topic have been published, including the three well-recognized texts on flow induced vibrations of pipe by Blevins (1990), Chen (1987) and Sümer & Fredsoe (1997).

Oz & Boyaci (2000) solved transverse vibrations of tensioned pipes conveying fluid with time-dependent velocity. Öz & Pakdemirli (1999); Öz, Pakdemirli, Boyacı (2001); Öz, Pakdemirli, Özkaya (1998); gave a good solution technique, multiple time scale perturbation method, for axially moving beam. The numerical solution of the mathematical model using finite differences was calculated by Semercigil, Turan & Lu (1997). Those both solution techniques are used extensively in this thesis.

1.2 Marine Pipelines

Pipeline stability in critical areas of unstable and/or rapidly developing morphology is a problem of vital importance not to be unnoticed in every pipeline project. Various environmental and natural hazards with potential risks of important damage to submarine pipelines may exist along a selected pipeline route. A considerable number of pipeline damages have occurred because of unforeseen and sudden changes of the original morphology of the sea floor on which they lay.

Environmental and natural hazards can be classified into two main categories: hazards that pre-exist and can be encountered during the pipeline installation on the seabed and during its planned operational life. The specific hazards and severity of these hazards depend on the pipeline-site location, while the protection works to be performed and the corrective actions to be taken depend mainly on the water depth and on the type of hazard. The pipeline may be exposed to mud slides and turbidity currents as well as to potential severe storm consequences induced under water and other major bottom instabilities. In the near shore areas, the pipeline normally exposed to high hydrodynamic forces and actions if it is just established on the seabed without any protective trenching. In other areas, depending on local situations and conditions, pipelines may have to be designed and installed considering earthquakes as well as active faulting which may occur in the area. When installed across straits, channels and narrow seas communicating with larger basins, pipelines may be subject to strong bottom currents, migration and collapse of dunes and sand waves, slumps and other slope instabilities. When laid across wide areas of shallow or relatively shallow waters, the pipeline is very likely to rest across a sequence of aggradation bedforms and sedimentary rhythmic mounded obstruction and parallel depressions that may cause unsupported free spans to the possible extent. Sand waves, dunes and other large, current generated bedforms with a ripple shape may become a major problem in the stability and protection of pipelines crossing wide seabed areas where these structures are presented and subject to current induced

migration. One of the most critical and still uncertain questions to geotechnical and construction engineers is the stability of these larger bedforms in relationship with the pipelines and the related offshore installation they support.

Basic criteria for the choice of the most proper and safest pipeline route across unstable areas also include the following concepts: minimize pipe length in unstable seafloors and route the pipeline in a relatively more stable area. In mud-flow areas, minimize any soil movement and slump risks of damage to the pipeline by routing the pipe in such a way that it runs in the same direction as the ascertained or most probable mud flow. This can normally be achieved by having the pipeline routed in a direction perpendicular to the bottom depth contours in the area.

To reduce potential risk of damage to the pipeline, the environmental threats must first be identified in the specific site, then measures be taken to protect the pipeline from these threats. The protection methods include trenching the pipeline below the seabed, anchoring of the pipeline, increased concrete coating, installation of supports installation of load/ protection mattress, gravel dumping and strengthening the pipeline. In the selection and the application of the most adequate and effective protection method, water depth plays a relevant role as a determining factor.

For stability and protection against mechanical damages, most offshore pipelines depend on the application of concrete coating of variable thickness. The design thickness of the concrete coating based on factors such as seabed currents, pipeline, size, buoyancy, concrete density, required corrosion protection and resistance to mechanical damage and spanning. Natural irregularities in the seabed topography, geomorphic discontinuities or scour under the pipeline during service normally result in substantial free lengths of unsupported pipeline which cannot be tolerated, as the concrete coating turns into overstressed and spans leading to loss of protection and instability and eventually to lasting damages to the pipeline structure. In common practice freespan reduction and correction is attained by providing intermediate supports, augmented where necessary by additional weight and perimeter protection.

Melegari&Bressan (1990) presented some pipeline support types in their paper.

Sandbags: Sandbagging is carry out to support free spans of cover exposed pipelines. It is very often the simplest and most cost valuable method for depths down to 50 mt.

Experiences and tests have shown that the conventional sandbags give a rather low level of protection against mechanical damage, while using sand/cement mixtures has been effective.



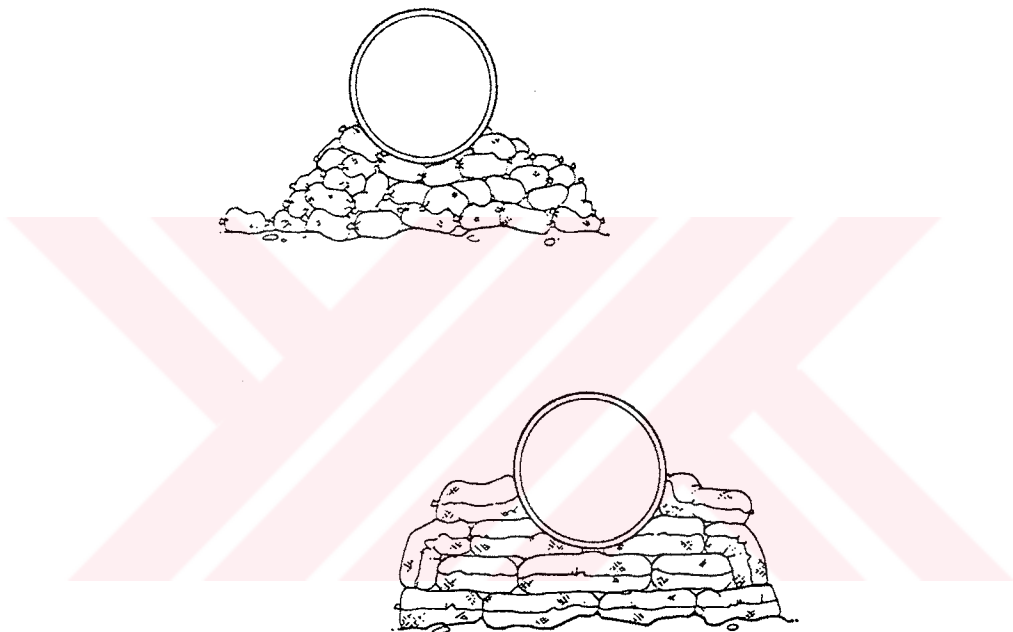
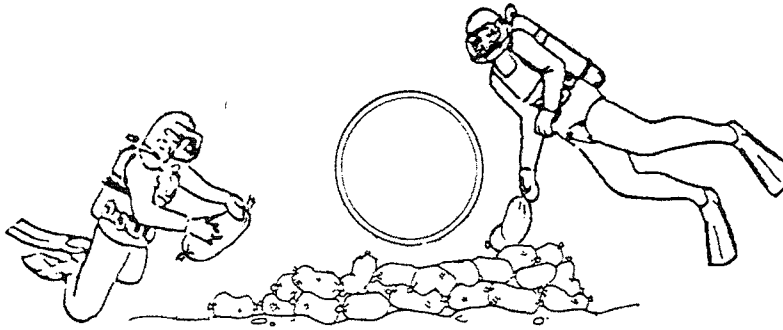


Figure 1.1 Sandbagging [Melegari&Bressan (1990)]

Grouting (support): This engineering solution is installed by hyperbaric divers under normal and technical conditions. It is based on a well-proven flexible fabric that is constructed to form bags or mattresses when filled with cement grout. The formwork is made from a purposewoven polypropylene fabric, the support/underpin form being based on several interconnected compartments with vent pipes to ensure proper filling and maintenance of contact with the underside of the pipeline for a standard distance/clearance. The system is modified to inflate the pipeline and the bags can be adapted to accommodate varying heights of undercut beneath the

pipeline. The filling grout is pumped from the surface support vessel through a grout umbilical consisting of two pressure hoses that provide a return line to the surface in order that the grout can be recirculated when necessary.

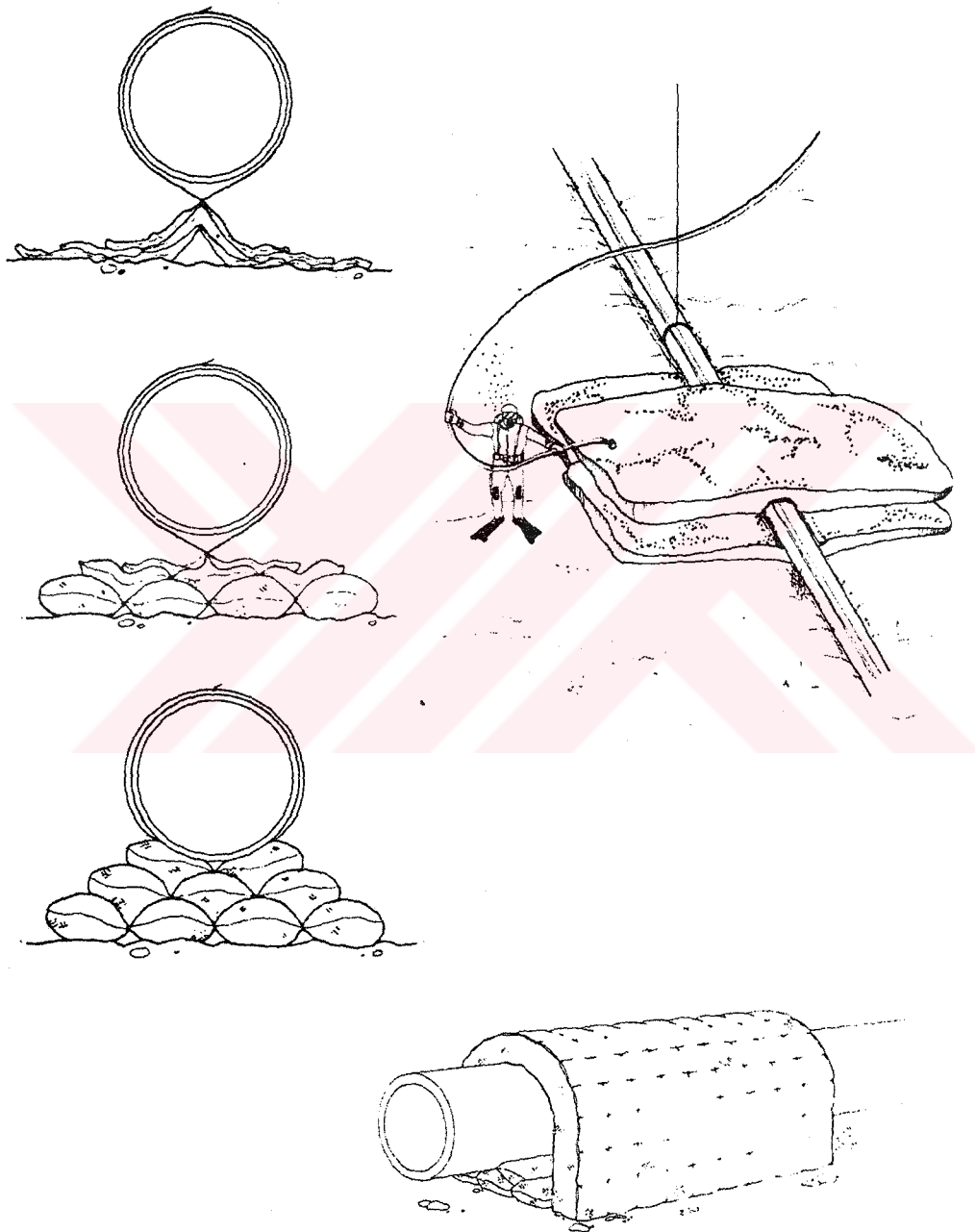


Figure 1.2 Grouting (support) [Melegari&Bressan (1990)]

Jack-ups (mechanical supports): In numerous cases specially designed active supports have been utilized to reduce the length of free spans with variable bottom clearance. The supports can adapt themselves perfectly to unevenness of the seabed by means of releasable legs. They are equipped with hydraulic jacks and compressed air cylinders that allow the pipe to be jacked-up so that it has an optimal configuration and stress position. In this case these supports become active supports. These types of supports are today suitable for installation at depths exceeding 500m.



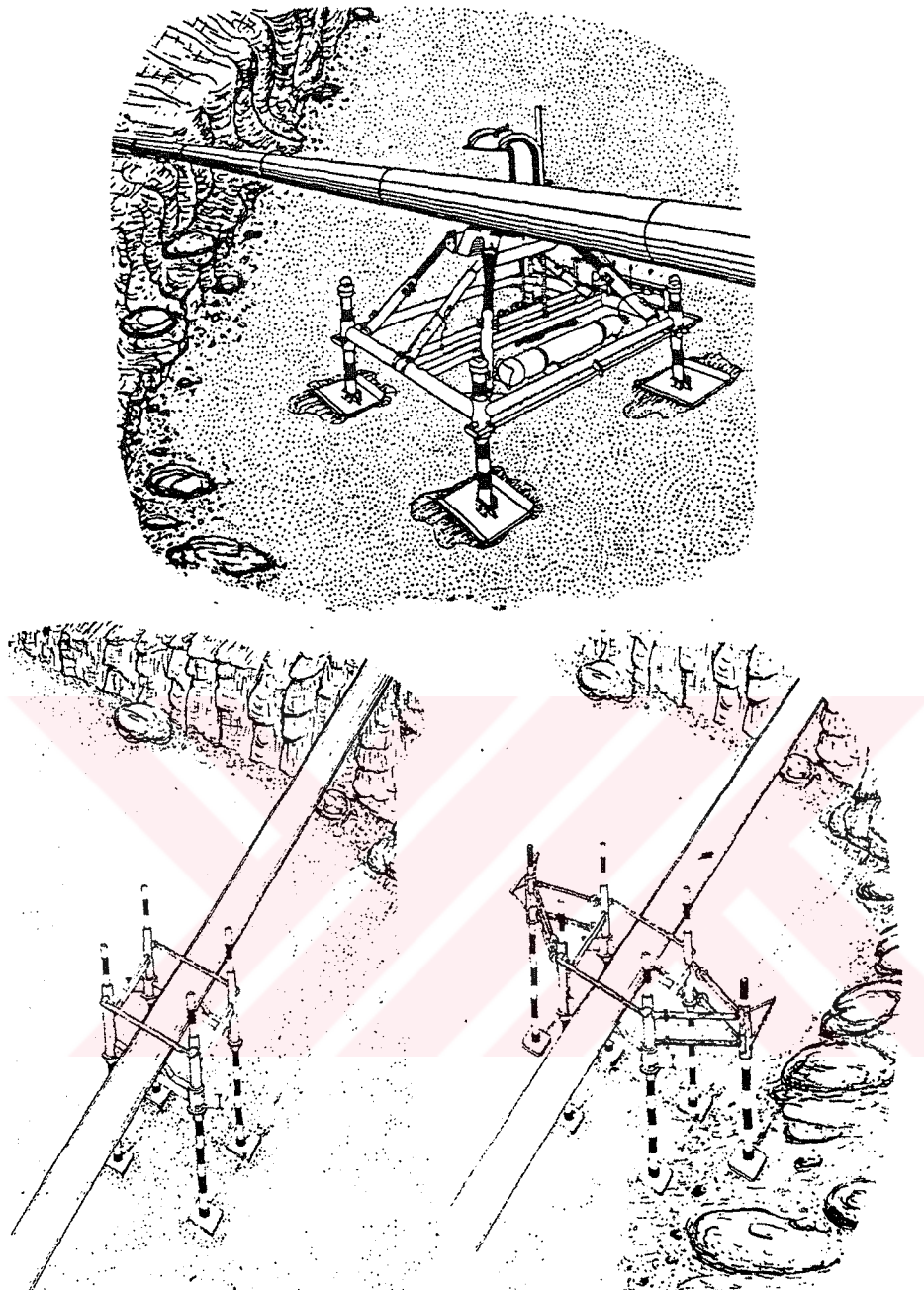


Figure 1.3 Jack ups (mechanical supports) [Melegari&Bressan (1990)]

Gravel dumping (backfilling): This method extensively used for correcting free spans. In this method a free span can be covered along its total length or only at certain points by forming heaps of material. Gravel backfilling can also be employed in combination with pipeline steel supports. The practice is to cover the supports

after installation so as to supply more stability and protection from erosion under supports themselves.

One important factor for the engineered backfilling is to determine the correct mixture and grain size of the backfill material. The backfill material must remain in place during the distinct environmental conditions that may occur. Also, it must not prevent fishing with seafloor towed fishing gears in the area.

Grouting (protection): The fabric formwork used for the installation of grouted supports can also be customized in the form of a saddlebag to provide additional weight coating or protection over the pipeline. In such conditions the same fabric material is tailored and adapted to suit the pipeline size, height from the seabed and definite weight.

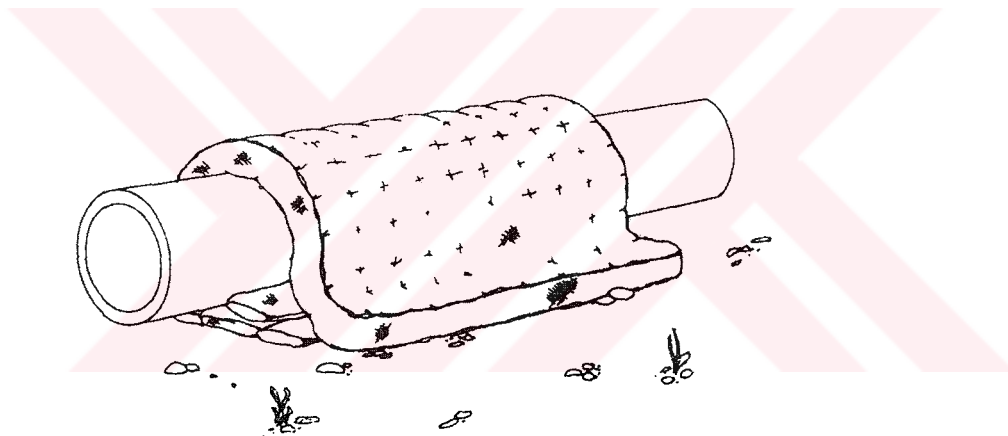


Figure 1.4 Grouting (protection) [Melegari&Bressan (1990)]

Bitumen mattresses: Bitumen mattresses are considered more suitable for the protection/stabilization of exposed parts of pipelines in deep water. Whenever an unsupported span is of considerable length and its clearance from the seabed is very little (centimeters), increasing the pipe's negative buoyancy on condition that it is maintained within the allowable stress limits can attain its correction. These mattresses can also be used in combination with other techniques, whenever negative reactions in the pipeline are necessary. Bitumen mattresses, to be wholly effective, need to be appropriately sized in relation to pipeline diameter. They are exceptionally

heavy for their size and with their flexibility; they can provide a very successful cure to difficult stabilization problems. The bituminous filler together with dense aggregates is used to provide weight, flexibility and long fixed protection to the pipeline.

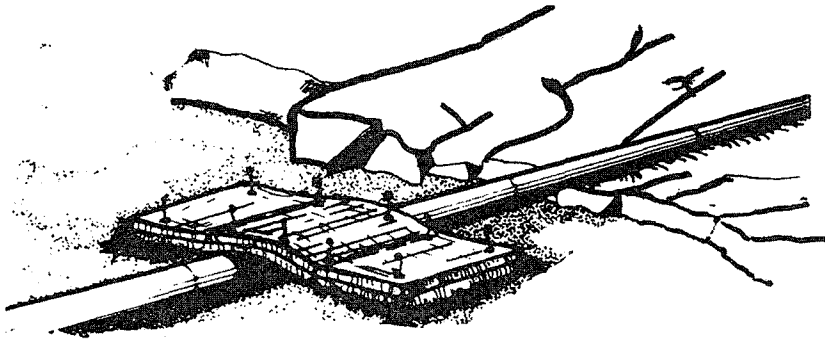


Figure 1.5 Bitumen mattress [Melegari&Bressan (1990)]

Concrete mattresses: These mattresses are constructed from reinforced concrete bars interconnected by steel or polypropylene ropes that give flexibility and capability to cope with an uneven seabed profile. This type of protection is appropriate for multiple applications in remedial works of pipelines and in the prevention of scour.

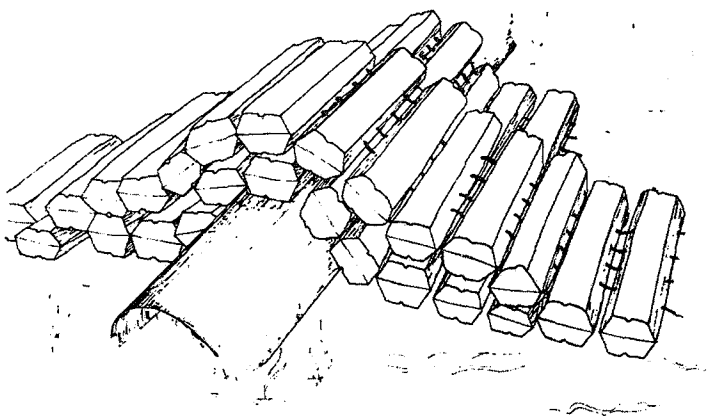


Figure 1.6 Concrete mattress [Melegari&Bressan (1990)]

Concrete saddles: Concrete saddles can be employed instead of sub mattresses to ensure added weight coating and protection on the pipeline and to protect it from local mechanical damages. These saddles are appropriate for repair of weight coating and local scour prevention. They clearly provide good mechanical protection to a pipeline and can be easily installed by divers or remotely controlled vehicle.

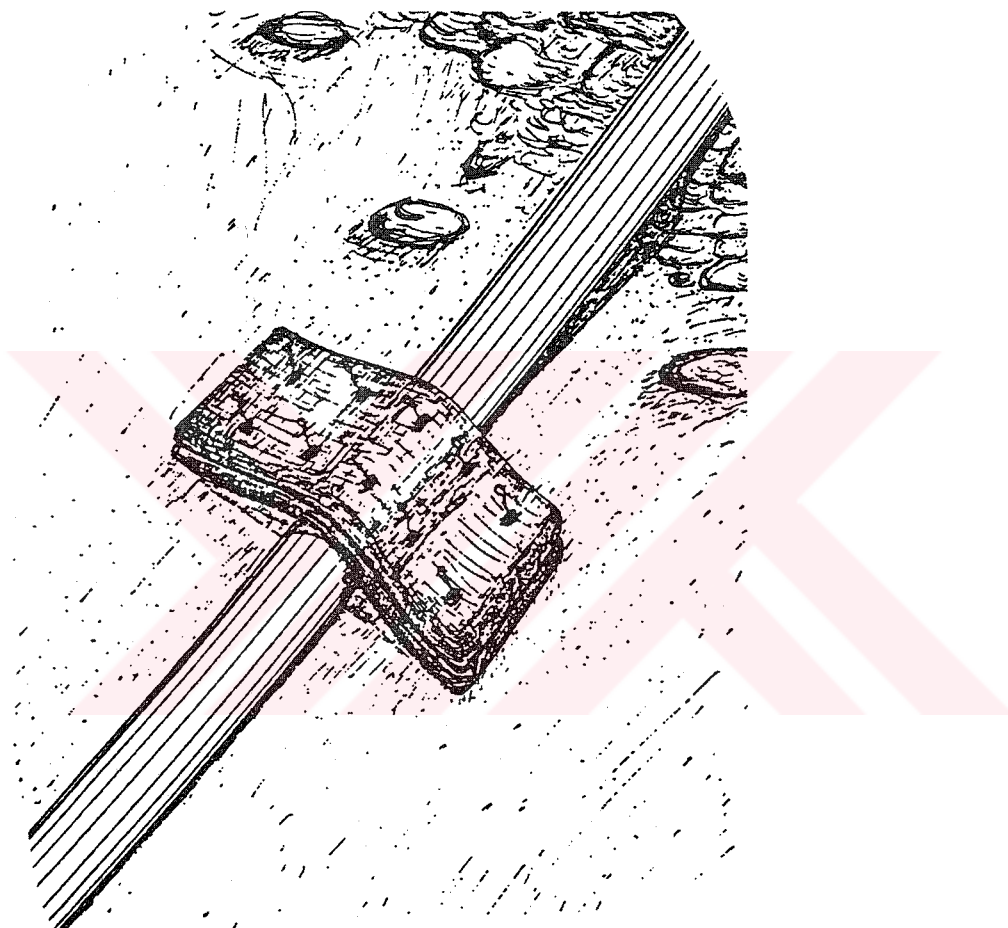


Figure 1.7 Concrete saddle [Melegari&Bressan (1990)]

Anchoring systems: In critical regions of pipeline, such as a shore approach or close to platforms, it may be necessary to anchor the pipeline by physically fixing it to the seabed to eliminate longitudinal or lateral movements. Two piles are driven into the bottom, one on each side of the pipeline, and a clamp is fitted around the top of the pipe and to the piles. This system is independent of the seabed soil because the

anchors can be pilled, drilled or screwed to the depth required to satisfy adequate restraint.

Pipes can today be generally grouped into two fundamental constrictions: The “Bounded” and “Non-Bounded”. Bounded pipes are those in which layers are applied and are chemically bonded to each other using bonding agents and special adhesive. “Non-Bounded” pipes are constructed using alternating layers of polymers, steel and flat wire reinforcement surrounded by tape or textile materials.

In the past five decades, pipes have been employed extensively in numerous offshore engineering applications. The most vital functions of them is to transport fluids drilled from underneath ocean floor such as oil, gas, hydrocarbon and their crude resources, up to the production platform or drilling ship and to discharge wastewater into sea, for examples, Hansen and Nedergaard (1982); Hansen & Fines (1982); Chucheepsakul, Monprapussorn and Huang (2003).

It is the objective of the paper [Chucheepsakul, Monprapussorn and Huang (2003)]: first to introduce mathematical principles for large strain analysis of extensible flexible marine pipes conveying fluid, second to show how to formulate large strain models of marine pipes in Cartesian and natural coordinates, and finally to illustrate versatile and sophisticated models suitable for two dimensional large strain analysis of extensible marine pipes conveying fluid.

1.3. Statement of the Problem

For the design of a piping system, the pipe supports have very important design features in consideration of resisting system load such as dead weights, thermal expansion, pump pulsation, water hammering and earthquakes. Piping systems such as the steam generator heat exchanger tubes, the main steam pipes and hot/cold leg pipes in a nuclear steam supply system, oil pipe lines, pump discharge lines, and marine risers, are supported in various ways, depending on environmental conditions

and individual requirements. Generally, the steam generator heat exchanger tubes and oil pipelines are planned with periodic support patterns.

Pakdemirli firstly used the non-ideal boundary conditions term in the literature. Types of support conditions in analysis of vibration of continuous systems such as beam, pipe, etc. are important and have direct effect on the solutions and natural frequency of system. Boundary conditions of real system are idealized with some assumptions by different type of supports. The real system is modeled by choosing one of the most suitable ideal boundary conditions. It is always assumed that those chosen ideal conditions satisfy the real system exactly. However, some small deviations from ideal conditions occur indeed in real systems. For example, a pipe connected at its ends to rigid supports by pins is modeled using simply supported boundary conditions that require deflections and moments to be zero. *However, the hole and pin assembly may have small gaps and/or friction which may introduce small deflections and/or moments at the ends. Similarly, a real built-in beam may have very small variations in deflection and/or slope. These types of boundary conditions with small deviations from the ideal conditions are defined as non-ideal boundary conditions,* Pakdemirli & Boyacı (2001 and 2002).

In this study, vibrations of the pipe having non-ideal boundary conditions with constant internal flow velocity for two different types of supported systems were analyzed. Using the perturbations (the Multiple Time Scale technique), the non-ideal boundary conditions are modeled. The idea is applied to two pipe vibration problems; fixed-fixed and clamped-clamped pipe. Effect of non-ideal boundary conditions on the natural frequencies and mode shapes are examined for each case using the Multiple Time Scale technique (MTST). The solution of this technique is compared with the finite difference method.

In this study, the equation of motion is derived using Hamilton's principle and then it is rewritten in non-dimensionalized form in Chapter 2. The flow velocity in the pipe is considered as constant and two types supported systems are analyzed with using MTST in Chapter 3. The non-ideal conditions introduce a type of non-linearity.

Therefore, to obtain solutions, some assumptions on non-ideal conditions have to be considered. The method of MTST is applied to the equation of motion in search of approximate solutions. In Chapter 4, the equation of motion is computed by the FDM. For some specific situation chosen among infinity problems are calculated by FDM.



CHAPTER TWO

THE EQUATION OF MOTIONS

2.1. The Equation of Motions

For the clamped-clamped and fixed-fixed pipes conveying fluid, x^* and y^* are the spatial co-ordinates, so y^* shows transverse displacements. v^* is the constant fluid velocity, ρ_f is the fluid density, A_p and A_f are the cross-sectional areas of the pipe and fluid and assumed to be constant. The length is L . The module of elasticity of the pipe is E_p . The transverse displacement is assumed to be small compared with the span L . The extensional stiffness of pipes is sufficiently large so that the longitudinal deformation is negligible. Variation of cross-sectional dimensions during vibrations of pipe is not considered. The gravity and fluid friction effects are neglected. Let us denote the time by t^* , the dot denotes differentiation with respect to time and the prime denotes differentiation with respect to the spatial variable x^* .

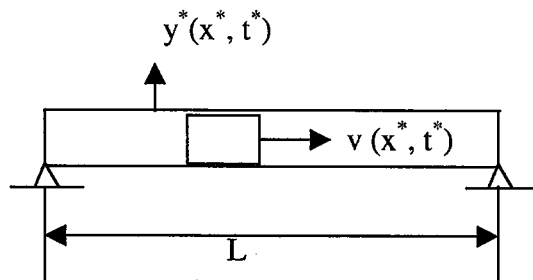


Figure 2.1 Schematics of translating continua in a pipe with fixed-fixed supports

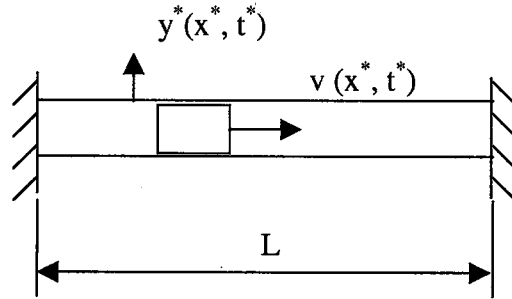


Figure 2.2 Schematics of translating continua in a pipe with clamped-clamped supports

The kinetic energy of the fluid is

$$T_f = \frac{1}{2} \rho_f A_f \int_0^L \left(\dot{y}^* + y^* v \right)^2 dx^* \quad (2.1)$$

The kinetic energy of the pipe is

$$T_p = \frac{1}{2} \rho_p A_p \int_0^L \left(\dot{y}^* \right)^2 dx^* \quad (2.2)$$

The total kinetic energy of the system is

$$T = \frac{1}{2} \rho_f A_f \int_0^L \left(\dot{y}^* + y^* v \right)^2 dx^* + \frac{1}{2} \rho_p A_p \int_0^L \left(\dot{y}^* \right)^2 dx^* \quad (2.3)$$

where the first term denotes the kinetic energies of the fluid in the y^* direction, the last term is the kinetic energy of the pipe in the y^* direction. The elastic energy of the system

$$U = \frac{1}{2} \int_0^L EI (y^{*''})^2 dx^* \quad (2.4)$$

The Lagrangian of the system is

$$\mathcal{L} = T - U \quad (2.5)$$

Hamilton's principle is

$$\delta \int_{t_1}^{t_2} \mathcal{L} dt^* = 0 \quad (2.6)$$

Substituting Equations (2.3) and (2.4) into Equation (2.5) and applying Hamilton's principle, Eq. (2.6), we can find

$$\delta \int_{t_1}^{t_2} \int_0^L \left\{ \frac{1}{2} \rho_f A_f \left(\dot{y}^* + y^{*'} v \right)^2 + \frac{1}{2} \rho_p A_p \dot{y}^{*2} - \frac{1}{2} EI y^{*''2} \right\} dx^* dt^* = 0 \quad (2.7)$$

Equation (2.7) can be rewritten in this form

$$I = \delta \int_{t_1}^{t_2} \int_0^L F \left(x^*, t^*, y, y', y'', \dot{y} \right) dx^* dt^* = 0 \quad (2.8)$$

where $F \left(x^*, t^*, y, y', y'', \dot{y} \right)$ is a known real function F of the real arguments x^*, y^*, t^* . The value of the integral depends on the choice of $y^* = y^*(x^*, t^*)$. We use the term functional to describe functions defined by integrals whose arguments themselves are functions.

$$\frac{\partial F}{\partial y} - \frac{\partial}{\partial x} \left(\frac{\partial F}{\partial y'} \right) + \frac{\partial^2}{\partial x^2} \left(\frac{\partial F}{\partial y''} \right) - \frac{\partial}{\partial t} \left(\frac{\partial F}{\partial \dot{y}} \right) = 0 \quad (2.9)$$

is a necessary condition that the integral, Equation(2.8), be minimized by $y = y(x^*, t^*)$. Equation (2.9) is the Euler equation associated with the variational problems for two independent and a dependent variables.

$$\frac{\partial F}{\partial y} = 0, \quad \frac{\partial F}{\partial y'} = \rho_f A_f v \left(\dot{y} + y' v \right), \quad \frac{\partial F}{\partial y''} = -EI y'' \quad (2.10)$$

$$\frac{\partial F}{\partial \dot{y}} = \rho_f A_f v \left(y + y' v \right) + \rho_p A_p \dot{y}$$

Substituting above derivations into equation (2.9), we can find equation of motion of pipes conveying fluid without viscous damping term and foundation modules.

$$EI \frac{\partial^4 y^*}{\partial x^{*4}} + \rho_f A_f v^2 \frac{\partial^2 y^*}{\partial x^{*2}} + 2\rho_f A_f v \frac{\partial^2 y^*}{\partial x^* \partial t^*} + m \frac{\partial^2 y^*}{\partial t^{*2}} = 0 \quad (2.11)$$

where m is $\rho_f A_f + \rho_p A_p$.

The various terms in Equation (2.11) may be identified, sequentially, as the flexural restoring force, a centrifugal term, a Coriolis term, and the inertia term. It is clear that the centrifugal force in Equation (2.11) acts as a compressive load. "In this way, it is easy to see and understand physically that, with increasing v , the effective stiffness of the system is diminished; for sufficiently large v , the destabilizing centrifugal force may overcome the restoring flexural force, resulting divergence, vulgarly known as buckling, and is some other circles as a pitchfork (static cusp) bifurcation." Paidoussis and Li (1993).

When we consider adding viscous damping, foundation modules and force terms, Equation (2.11) transforms

$$EI \frac{\partial^4 y^*}{\partial x^{*4}} + \rho_f A_f v^2 \frac{\partial^2 y^*}{\partial x^{*2}} + 2\rho_f A_f v \frac{\partial^2 y^*}{\partial x^* \partial t^*} + ky^* + \lambda \frac{\partial y^*}{\partial t^*} + m \frac{\partial^2 y^*}{\partial t^{*2}} = f \quad (2.12)$$

2.2. Non-dimensionalized of the Equation

The equation of motion will be non-dimensionalized since we can solve the problem in a way that is independent from size and type of material. The equation can be non-dimensionalized by substituting

$$y = y^* / L, x = x^* / L, t = t^* \sqrt{EI / mL^4} \quad (2.13)$$

we can write:

$$\frac{\partial y^*}{\partial t^*} = \frac{\partial(y.L)}{\partial t} \frac{\partial t}{\partial t^*} = \sqrt{\frac{EI}{mL^2}} \frac{\partial y}{\partial t} \quad (2.14)$$

below terms can be find in similar way

$$\frac{\partial^2 y^*}{\partial t^{*2}} = \frac{EI}{mL^3} \frac{\partial^2 y}{\partial t^2} \quad (2.15)$$

$$\frac{\partial^2 y^*}{\partial x^* \partial t^*} = \sqrt{\frac{EI}{mL^4}} \frac{\partial^2 y}{\partial x \partial t} \quad (2.16)$$

$$\frac{\partial y^*}{\partial x^*} = \frac{\partial y}{\partial x} \quad (2.17)$$

$$\frac{\partial^2 y^*}{\partial x^{*2}} = \frac{1}{L} \frac{\partial^2 y}{\partial x^2} \quad (2.18)$$

$$\frac{\partial^4 y^*}{\partial x^{*4}} = \frac{1}{L^3} \frac{\partial^4 y}{\partial x^4} \quad (2.18)$$

substituting equations from (2.13) to (2.18) into equation (2.12), we obtain

$$\underbrace{\frac{\partial^4 y}{\partial x^4}}_{(I)} + \underbrace{V^2 \frac{\partial^2 y}{\partial x^2}}_{(II)} + \underbrace{2\sqrt{\beta V} \frac{\partial^2 y}{\partial x \partial t}}_{(III)} + \underbrace{Ky}_{(IV)} + \underbrace{\mu \frac{\partial y}{\partial t}}_{(V)} + \underbrace{\frac{\partial^2 y}{\partial t^2}}_{(VI)} = \underbrace{F}_{(VII)} \quad (2.20)$$

where $\beta = \rho A / m$, $V = vL\sqrt{\rho_f A_f / EI}$, $K = k \frac{L^4}{EI}$, $\mu = \lambda L^2 / \sqrt{mEI}$, and

$$F = f \frac{L^3}{EI}$$

Terms (I) and (VI) constitute the simple beam equation, while (II) and (III) are the curvature term (or the centrifugal term) and the Coriolis force term, respectively. Term (IV) represents linear elastic foundations. The structural damping is represented with term (V) in Equation (2.20). V is the non-dimensional flow velocity term and the effect of the flow is reflected by parameters V and β . (Semercigil et al., 1997)

CHAPTER THREE

SOLUTIONS OF THE EQUATION OF MOTION
FOR NON-IDEAL BOUNDARY CONDITIONS

3.1 Introduction

In this chapter we will solve Equation (2.20.) without foundation terms (IV) under the nonlinear boundary conditions, which is called non-ideal boundary conditions. It means that the pipes are not lying on elastic foundations. The viscous damping coefficient in the term (V) assumed to be so small. So we will consider this term in below form

$$\varepsilon\mu \frac{\partial y}{\partial t}$$

and we accept no external force acting on pipes. Now, Equation (2.20) changes into below form

$$\underbrace{\frac{\partial^4 y}{\partial x^4}}_{(i)} + V^2 \underbrace{\frac{\partial^2 y}{\partial x^2}}_{(ii)} + 2\sqrt{\beta}V \underbrace{\frac{\partial^2 y}{\partial x \partial t}}_{(iii)} + \varepsilon\mu \underbrace{\frac{\partial y}{\partial t}}_{(v)} + \underbrace{\frac{\partial^2 y}{\partial t^2}}_{(vi)} = 0 \quad (3.1)$$

3.2 Solution for Fixed-Fixed Pipes

Here one may assume that both of the boundary conditions are non-ideal or only one is non-ideal. Now here both side boundary conditions will be taken as non-ideal. Hence, the non-ideal boundary conditions for the fixed- fixed pipe are

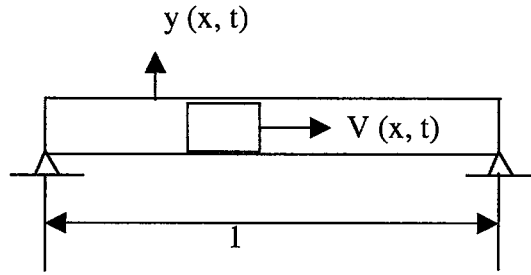


Figure 3.1 Schematics of translating continua in a pipe with fixed-fixed supports

$$y(0, t) = \varepsilon a(t), \quad y(l, t) = \varepsilon b(t) \quad (3.2)$$

and the other conditions are

$$y''(0, t) = 0, \quad y''(l, t) = 0 \quad (3.3)$$

Contrary to the pipe problems with ideal boundaries, variations in the displacements at the boundaries affect frequencies as well as amplitudes. The method of Multiple Time Scales is employed in search of approximate solutions.

The following expansion is assumed

$$y(x, t; \varepsilon) = y_0(x, T_0, T_1) + \varepsilon y_1(x, T_0, T_1) \quad (3.4)$$

where $T_0=t$ is the fast time scale and $T_1=\epsilon t$ is the slow time scale. Time derivatives are defined as

$$\frac{d}{dt} = D_0 + \epsilon D_1 + \dots, \quad \frac{d^2}{dt^2} = D_0^2 + 2\epsilon D_0 D_1 + \dots, \quad (3.5)$$

where $D_n = \partial / \partial T_n$. Substituting Equations (3.4) and (3.5) into Equation (3.1)

$$\begin{aligned} & y_0'' + \epsilon y_1'' + V^2 (y_0'' + y_1'') + 2\sqrt{\beta}V [(y_0' + \epsilon y_1')(D_0 + \epsilon D_1)] \\ & + \epsilon \mu [(y_0 + \epsilon y_1)(D_0 + \epsilon D_1)] + (y_0 + \epsilon y_1)(D_0^2 + 2\epsilon D_0 D_1) = 0 \end{aligned} \quad (3.6)$$

now, separating terms at each order of ϵ , one obtains

$$\begin{aligned} & O(1): \\ & y_0'' + V^2 y_0'' + 2\sqrt{\beta}V D_0 y_0' + D_0^2 y_0 = 0 \\ & y_0(0, T_0, T_1) = y_0(1, T_0, T_1) = 0 \end{aligned} \quad (3.7)$$

$$\begin{aligned} & O(\epsilon): \\ & y_1'' + V^2 y_1'' + 2\sqrt{\beta}V D_0 y_1' + D_0^2 y_1 = -2\sqrt{\beta}V D_1 y_0' - \mu D_0 y_0 - 2D_0 D_1 y_0 \\ & y_1(0, T_0, T_1) = a(T_0, T_1), y_1(1, T_0, T_1) = b(T_0, T_1) \end{aligned} \quad (3.8)$$

The solution at order 1 can be written as follows:

$$y_0(x, T_0, T_1; \epsilon) = A_n(T_1) e^{i\omega_n T_0} Y_n(x) + \bar{A}_n(T_1) e^{i\omega_n T_0} \bar{Y}_n(x) \quad (3.9)$$

substituting Equation (3.9) into the equation at order 1, the spatial functions $Y_n(x)$ satisfy the equation

$$Y_n'' + V^2 Y_n'' + 2i\omega_n \sqrt{\beta}V Y_n' - \omega_n Y_n = 0 \quad (3.10)$$

with the boundary conditions

$$Y_n(0)=0, Y_n(1)=0, Y_n''(0)=0, Y_n''(1)=0 \quad (3.11)$$

The solution of $Y_n(x)$ is

$$Y_n(x) = c_{1n} \left(e^{i\alpha_{1n}x} + C_{2n} e^{i\alpha_{2n}x} + C_{3n} e^{i\alpha_{3n}x} + C_{4n} e^{i\alpha_{4n}x} \right) \quad (3.12)$$

substituting this equation into Eq. (3.10)

$$\begin{aligned} & c_{1n} \left\{ \left[\alpha_{1n}^4 - V^2 \alpha_{1n}^2 - 2\omega_n \sqrt{\beta V} \alpha_{1n} - \omega_n^2 \right] e^{i\alpha_{1n}x} \right. \\ & + \left[\alpha_{2n}^4 - V^2 \alpha_{2n}^2 - 2\omega_n \sqrt{\beta V} \alpha_{2n} - \omega_n^2 \right] C_{2n} e^{i\alpha_{2n}x} \\ & + \left[\alpha_{3n}^4 - V^2 \alpha_{3n}^2 - 2\omega_n \sqrt{\beta V} \alpha_{3n} - \omega_n^2 \right] C_{3n} e^{i\alpha_{3n}x} \\ & \left. + \left[\alpha_{4n}^4 - V^2 \alpha_{4n}^2 - 2\omega_n \sqrt{\beta V} \alpha_{4n} - \omega_n^2 \right] C_{4n} e^{i\alpha_{4n}x} \right\} = 0 \end{aligned} \quad (3.13)$$

one obtain the dispersive relation

$$\alpha_{jn}^4 - V^2 \alpha_{jn}^2 - 2\omega_n \sqrt{\beta V} \alpha_{jn} - \omega_n^2 = 0 \quad j=1,2,3,\dots, \quad n=1,2,3,\dots \quad (3.14)$$

The α_{jn} satisfy Equation (3.14). Applying boundary conditions (3.11) to dispersive relation, one obtain four equations those are

From $Y_n(0) = 0$,

$$c_{1n} (1 + C_{2n} + C_{3n} + C_{4n}) = 0 \quad (3.15)$$

from $Y_n''(0) = 0$,

$$c_{1n} (\alpha_{1n}^2 + C_{2n} \alpha_{2n}^2 + C_{3n} \alpha_{3n}^2 + C_{4n} \alpha_{4n}^2) = 0 \quad (3.16)$$

from $Y_n(1) = 0$,

$$c_{1n} \left(e^{i\alpha_{1n}} + C_{2n} e^{i\alpha_{2n}} + C_{3n} e^{i\alpha_{3n}} + C_{4n} e^{i\alpha_{4n}} \right) = 0 \quad (3.17)$$

from $Y_n''(1) = 0$,

$$c_{1n} \left(\alpha_{1n}^2 e^{i\alpha_{1n}} + C_{2n} \alpha_{2n}^2 e^{i\alpha_{2n}} + C_{3n} \alpha_{3n}^2 e^{i\alpha_{3n}} + C_{4n} \alpha_{4n}^2 e^{i\alpha_{4n}} \right) = 0 \quad (3.18)$$

now, applying the boundary conditions to the solution, the matrix equation is obtained as follows

$$\begin{bmatrix} 1 & 1 & 1 & 1 \\ \alpha_1^2 & \alpha_2^2 & \alpha_3^2 & \alpha_4^2 \\ e^{i\alpha_1} & e^{i\alpha_2} & e^{i\alpha_3} & e^{i\alpha_4} \\ \alpha_1^2 e^{i\alpha_1} & \alpha_2^2 e^{i\alpha_2} & \alpha_3^2 e^{i\alpha_3} & \alpha_4^2 e^{i\alpha_4} \end{bmatrix} \begin{Bmatrix} 1 \\ C_{2n} \\ C_{3n} \\ C_{4n} \end{Bmatrix} c_{1n} = \begin{Bmatrix} 0 \\ 0 \\ 0 \\ 0 \end{Bmatrix} \quad (3.19)$$

for non-trivial solutions, the determinant of the coefficient matrix must be zero, which yields the support condition;

$$\begin{aligned} & \left[e^{i(\alpha_{1n} + \alpha_{2n})} + e^{i(\alpha_{3n} + \alpha_{4n})} \right] (\alpha_{1n}^2 - \alpha_{2n}^2) (\alpha_{3n}^2 - \alpha_{4n}^2) \\ & + \left[e^{i(\alpha_{1n} + \alpha_{3n})} + e^{i(\alpha_{2n} + \alpha_{4n})} \right] (\alpha_{2n}^2 - \alpha_{4n}^2) (\alpha_{3n}^2 - \alpha_{1n}^2) \\ & + \left[e^{i(\alpha_{2n} + \alpha_{3n})} + e^{i(\alpha_{1n} + \alpha_{4n})} \right] (\alpha_{1n}^2 - \alpha_{4n}^2) (\alpha_{2n}^2 - \alpha_{3n}^2) = 0 \end{aligned} \quad (3.20)$$

Numerical values of ω_n as well as α_{in} can be calculated by using Equations (3.14) and (3.20).

Now, to obtain C_{2n} , C_{3n} , C_{4n} coefficients, Equation (3.15) is multiplied with α_{4n}^2 and then subtracted from Equation (3.16)

$$c_{1n} \left[(\alpha_{4n}^2 - \alpha_{1n}^2) + C_{2n} (\alpha_{4n}^2 - \alpha_{2n}^2) + C_{3n} (\alpha_{4n}^2 - \alpha_{3n}^2) \right] = 0 \quad (3.21)$$

in similar way, Equation (3.17) is multiplying with α_{4n}^2 and obtained term is subtracted from Equation (3.18)

$$c_{1n} \left[(\alpha_{4n}^2 - \alpha_{1n}^2) e^{i\alpha_{1n}} + C_{2n} (\alpha_{4n}^2 - \alpha_{2n}^2) e^{i\alpha_{2n}} + C_{3n} (\alpha_{4n}^2 - \alpha_{3n}^2) e^{i\alpha_{3n}} \right] = 0 \quad (3.22)$$

using (3.21) and (3.22), C_{2n} , C_{3n} can be obtained. Firstly Equation (3.21) is multiplied $e^{i\alpha_{3n}}$ and then equation (3.22) is subtracted from this obtained term

$$c_{1n} \left[(\alpha_{4n}^2 - \alpha_{1n}^2) (e^{i\alpha_{3n}} - e^{i\alpha_{1n}}) + C_{2n} (\alpha_{4n}^2 - \alpha_{2n}^2) (e^{i\alpha_{3n}} - e^{i\alpha_{2n}}) \right] = 0 \quad (3.23)$$

C_{2n} can be driven from above equation

$$C_{2n} = \frac{(\alpha_{4n}^2 - \alpha_{1n}^2) (e^{i\alpha_{3n}} - e^{i\alpha_{1n}})}{(\alpha_{4n}^2 - \alpha_{2n}^2) (e^{i\alpha_{3n}} - e^{i\alpha_{2n}})} \quad (3.24)$$

Now again same operations is applied same equations but multiplying $e^{i\alpha_{2n}}$

$$c_{1n} \left[(\alpha_{4n}^2 - \alpha_{1n}^2) (e^{i\alpha_{2n}} - e^{i\alpha_{1n}}) + C_{3n} (\alpha_{4n}^2 - \alpha_{3n}^2) (e^{i\alpha_{2n}} - e^{i\alpha_{3n}}) \right] = 0 \quad (3.25)$$

and then

$$C_{3n} = \frac{(\alpha_{4n}^2 - \alpha_{1n}^2) (e^{i\alpha_{2n}} - e^{i\alpha_{1n}})}{(\alpha_{4n}^2 - \alpha_{3n}^2) (e^{i\alpha_{2n}} - e^{i\alpha_{3n}})} \quad (3.26)$$

The last coefficient is

$$C_{4n} = -1 - C_{2n} - C_{3n} \quad (3.27)$$

Now those coefficients are substituting into (3.12)

$$Y_n(x) = c_{1n} \left[e^{i\alpha_{1n}x} - \frac{(\alpha_{4n}^2 - \alpha_{1n}^2)(e^{i\alpha_{3n}} - e^{i\alpha_{1n}})}{(\alpha_{4n}^2 - \alpha_{2n}^2)(e^{i\alpha_{3n}} - e^{i\alpha_{2n}})} e^{i\alpha_{2n}x} - \frac{(\alpha_{4n}^2 - \alpha_{1n}^2)(e^{i\alpha_{2n}} - e^{i\alpha_{1n}})}{(\alpha_{4n}^2 - \alpha_{3n}^2)(e^{i\alpha_{2n}} - e^{i\alpha_{3n}})} e^{i\alpha_{3n}x} \right. \\ \left. + \left(-1 + \frac{(\alpha_{4n}^2 - \alpha_{1n}^2)(e^{i\alpha_{3n}} - e^{i\alpha_{1n}})}{(\alpha_{4n}^2 - \alpha_{2n}^2)(e^{i\alpha_{3n}} - e^{i\alpha_{2n}})} + \frac{(\alpha_{4n}^2 - \alpha_{1n}^2)(e^{i\alpha_{2n}} - e^{i\alpha_{1n}})}{(\alpha_{4n}^2 - \alpha_{3n}^2)(e^{i\alpha_{2n}} - e^{i\alpha_{3n}})} \right) e^{i\alpha_{4n}x} \right] \quad (3.27)$$

To find the solution at second order of approximation, one substitutes Equation (3.9) into the right-hand side of Equation (3.7). The result is

$$y_1^{iv} + V^2 y_1'' + 2\sqrt{\beta} V D_0 y_1' + D_0^2 y_1 = -2\sqrt{\beta} V Y_n' D_1 A_n e^{i\omega_0 T_0} - \mu i \omega_n Y_n A_n e^{i\omega_0 T_0} \\ - 2i \omega_n Y_n D_1 A_n e^{i\omega_0 T_0} + c.c. \quad (3.28)$$

where c.c. stands for complex conjugate of the preceding term. Assuming a solution of the following form:

$$y_1 = \psi_n(x, T_1) e^{i\omega_n T_0} + c.c. \quad (3.29)$$

and substituting into Equation (3.28) and boundary conditions in Equation (3.8), one has

$$\psi_n^{iv} + V^2 \psi_n'' + 2i \omega_n \sqrt{\beta} V \psi_n' - \omega^2 \psi_n = -2\sqrt{\beta} V Y_n' D_1 A_n - \mu i \omega_n Y_n A_n \\ - 2i \omega_n Y_n D_1 A_n \quad (3.30)$$

and

$$\begin{aligned}
y_1(0, T_0, T_1) &= \psi(0, T_1) e^{i\omega_n T_0} + c.c. = a_0 A(T_1) e^{i\omega_n T_0} + c.c., \\
y_1(1, T_0, T_1) &= \psi(1, T_1) e^{i\omega_n T_0} + c.c. = b_0 A(T_1) e^{i\omega_n T_0} + c.c.,
\end{aligned} \tag{3.31}$$

and then

$$\begin{aligned}
\psi(0, T_1) &= a_0 A(T_1), \\
\psi(1, T_1) &= b_0 A(T_1)
\end{aligned} \tag{3.32}$$

The homogeneous part of Equation (3.30) has a non-trivial solution. For the non-homogenous problem, to have a solution, a solvability condition should be satisfied. To find this condition multiply the equation by an unknown function $u_n(x)$ and integrate over the domain.

$$\begin{aligned}
\int_0^1 (\psi_n^{iv} + V^2 \psi_n'' + 2i\omega_n \sqrt{\beta V} \psi_n' - \omega^2 \psi_n) u dx &= \int_0^1 u (-2\sqrt{\beta V} Y_n' D_1 A_n) dx \\
&\quad - \int_0^1 u (\mu i \omega_n Y_n A_n) dx - \int_0^1 u (2i\omega_n Y_n D_1 A_n) dx
\end{aligned} \tag{3.33}$$

The right hand side of the equation is assumed zero. To transfer the differentiability from ψ_n to u_n , one use the integration-by-parts formula

$$\int_0^1 \psi_n' u_n dx = \left| \psi_n u_n \right|_0^1 - \int_0^1 \psi_n u_n' dx \tag{3.34a}$$

$$\int_0^1 \psi_n'' u_n dx = \left| \psi_n' u_n - \psi_n u_n' \right|_0^1 + \int_0^1 \psi_n u_n'' dx \tag{3.34b}$$

$$\int_0^1 \psi_n^{iv} u dx = \left| \psi_n''' u_n - \psi_n'' u_n' + \psi_n' u_n'' - \psi_n u_n''' \right|_0^1 + \int_0^1 \psi_n u_n^{iv} dx \tag{3.34c}$$

Substituting Equations (3.34) into Equation (3.30)

$$\int_0^1 \left(u_n^{iv} + V^2 u_n'' - 2i\omega_n \sqrt{\beta V} u_n' - \omega_n^2 u_n \right) \psi_n dx + \left(\psi_n'' u_n - \psi_n' u_n' + \psi_n' u_n'' - \psi_n u_n''' \right) \Big|_0^1 + V^2 \left(\psi_n' u_n - \psi_n u_n' \right) \Big|_0^1 + 2i\omega_n \sqrt{\beta V} \left(\psi_n u_n \right) \Big|_0^1 = 0 \quad (3.35)$$

Applying boundary conditions for the second order, one can find form of “ u_n unknown” function. Now looking at integration parts of above equation, one can say

$$u_n(x) = \overline{Y_n(x)}$$

It means $u_n(x)$ is equal to conjugate of $Y_n(x)$. Applying boundary conditions of (3.32) and using above terms Equation (3.30) can be rewritten below form:

$$\begin{aligned} & -\overline{Y_n}''(1) b_0 A_n(T_1) - V^2 \overline{Y_n}'(1) b_0 A_n(T_1) + \overline{Y_n}''(0) a_0 A_n(T_1) + V^2 \overline{Y_n}'(0) a_0 A_n(T_1) = \\ & -2\sqrt{\beta V} D_1 A_n(T_1) \int_0^1 Y_n' \overline{Y_n} - \mu i \omega_n A_n(T_1) \int_0^1 Y_n \overline{Y_n} - 2i\omega_n D_1 A_n(T_1) \int_0^1 Y_n \overline{Y_n} \end{aligned} \quad (3.36)$$

Rearranging (3.36), one can write an ordinary differential equation

$$D_1 A = \frac{b_0 \left(\overline{Y_n}''(1) + V^2 \overline{Y_n}'(1) \right) - a_0 \left(\overline{Y_n}''(0) + V^2 \overline{Y_n}'(0) \right) - \mu i \omega \int_0^1 Y_n \overline{Y_n} dx}{\underbrace{2\sqrt{\beta V} \int_0^1 Y_n' \overline{Y_n} dx + 2i\omega \int_0^1 Y_n \overline{Y_n} dx}_{Z=Z_1+iZ_2}} A \quad (3.37)$$

whose solution is

$$A(T_1) = C e^{ZT_1} = C e^{(Z_1+iZ_2)T_1} \quad (3.38)$$

where $C = ce^{i\theta}$ is a complex constant. θ and c are constants to be determined by initial conditions. For the ideal boundary conditions, $a_0 = b_0 = 0$, term Z is;

$$Z = \frac{-\mu i \omega \int_0^1 Y_n \bar{Y}_n dx}{2\sqrt{\beta V} \int_0^1 Y_n \bar{Y}_n dx + 2i\omega \int_0^1 Y_n \bar{Y}_n dx} \quad (3.39)$$

when there is no damping in the system, the solution of the system is transformed into at one order solution ($\varepsilon = 0$). Substituting back Equation (3.38) into Equation (3.9), returning to the original time variable

$$y_0(x, T_0, T_1; \varepsilon) = ce^{i\theta} e^{(Z_1 + iZ_2)T_1} e^{i\omega_n T_0} Y_n(x) + ce^{-i\theta} e^{(Z_1 - iZ_2)T_1} e^{-i\omega_n T_0} \bar{Y}_n(x) \quad (3.40)$$

and considering $T_0 = \varepsilon T_1$ and rearranging this term,

$$y_0(x, T_0; \varepsilon) = ce^{Z_1} \left(e^{i[(\omega_n + \varepsilon Z_2)T_0 + \theta]} Y_n(x) + e^{-i[(\omega_n + \varepsilon Z_2)T_0 + \theta]} \bar{Y}_n(x) \right) \quad (3.41)$$

where Z_2 is modifier frequency term due to the non-ideal boundary conditions and θ is phase angle. Returning to the original time, one finally obtains the approximate response as follows:

$$y_0(x, t) = ce^{Z_1} \left(e^{i[(\omega_n + \varepsilon Z_2)t + \theta]} Y_n(x) + e^{-i[(\omega_n + \varepsilon Z_2)t + \theta]} \bar{Y}_n(x) \right) \quad (3.42)$$

The frequency due to non-ideal boundary condition is

$$\omega_n = \omega_n + Z_2 \quad (3.43)$$

Non-ideal boundary condition is

$$y(0, t) = \varepsilon a_0 e^{z\varepsilon t}, \quad y(1, t) = \varepsilon b_0 e^{z\varepsilon t} \quad (3.44)$$

3.2.1 Numerical Results

The equation of motion and amplitude of vibration $A(T_1)$ term is rewritten as

$$\underbrace{\frac{\partial^4 y}{\partial x^4}}_{(i)} + V^2 \underbrace{\frac{\partial^2 y}{\partial x^2}}_{(ii)} + 2\sqrt{\beta}V \underbrace{\frac{\partial^2 y}{\partial x \partial t}}_{(iii)} + \epsilon\mu \underbrace{\frac{\partial y}{\partial t}}_{(v)} + \underbrace{\frac{\partial^2 y}{\partial t^2}}_{(vi)} = 0$$

$$D_1 A = \frac{b_0 \left(\overline{Y}_n''(1) + V^2 \overline{Y}_n'(1) \right) - a_0 \left(\overline{Y}_n''(0) + V^2 \overline{Y}_n'(0) \right) - \mu i \omega \int_0^1 \overline{Y}_n \overline{Y}_n' dx}{\underbrace{2\sqrt{\beta}V \int_0^1 \overline{Y}_n' \overline{Y}_n dx + 2i\omega \int_0^1 \overline{Y}_n \overline{Y}_n' dx}_{Z=Z_1+iZ_2}} A$$

Some parameters are present in these equations. Numerical results of equation of motion depend on parameters V , a_0 , b_0 , β , μ . In this section numerical results are given with respect to V , a_0 , b_0 in graphics form. Therefore, effects of these parameters on numerical results will be seen in below figures.

Square root of β parameter in range of 0 to 1 is in equation of motion and amplitude of vibration. Therefore, β has a small effect on numerical results. So, effect of variation of β is not illustrated in figures.

Effect of external damping coefficient on numerical results are plotted in Figures (3.4)-(3.5).

In Figures (3.2)-(3.3), y-axis represents the natural circular frequency of the vibration. It is customarily measured in radians per unit time. The natural frequency, ω , has varied through 2π radians. Hence, one can write

$$\tau = \text{Period of vibration} = 2\pi/\omega$$

The natural frequency, which is the reciprocal, is defined as

$$f = \frac{1}{\tau} = \frac{\omega}{2\pi} \text{ (hz)}$$

Where, time is in dimensionless form. To compute time in dimensional form Equation (2.11) can be used.

$$y = y^* / L, x = x^* / L, t = t^* \sqrt{EI / mL^4} \quad (2.11)$$

In figures, x-axis reflects non-dimensional flow velocity, V. Non-dimensional form of velocity can be obtained from the equation below. Also, if the non-dimensional velocity (V) is known and then its dimensional form can be calculated using the equation;

$$V = vL\sqrt{\rho_f A_f / EI}$$

In this section, the numerical examples will be given for the vibrations of pipes conveying fluid with non-ideal boundary conditions. In Figures (3.1-3.2), natural frequencies for fixed-fixed are given depending on velocity of fluid and amplitude of non-ideal boundary conditions for the first and second modes.

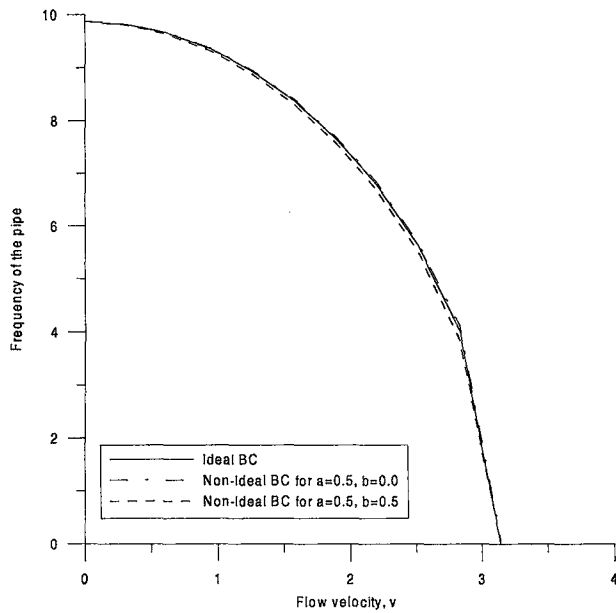


Figure 3.2 Comparisons of the first natural frequencies for different non-ideal boundary conditions for fixed-fixed supports ($\beta=0.8$, $\epsilon=0.1$, $\mu=1.0$)

Depending on the mode numbers and flow velocities, the frequencies, altered by non-ideal boundary conditions, may increase, decrease or remain unchanged. The natural frequencies decrease with increasing of the velocity. Variation of the ratio of fluid masses (fluid to pipe ratio) has small effect on the natural frequencies due to square root of it in the equation of motion. On the other hand, at higher modes, the natural frequency values increase. The ideal and non-ideal frequencies are drawn as a function of the flow velocity.

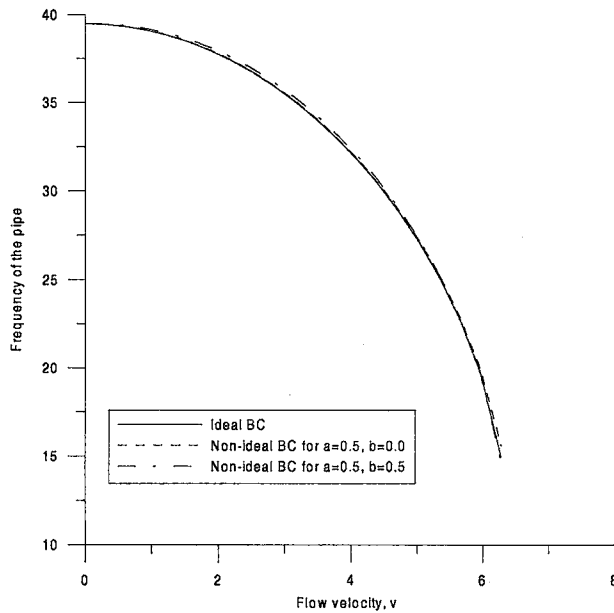


Figure 3.3 Comparisons of the second natural frequencies for different non-ideal boundary conditions for fixed-fixed supports ($\beta=0.8$, $\varepsilon=0.1$, $\mu=1.0$).

Another interesting feature of the non-ideal boundary conditions is growth or decay of the amplitudes depending on the argument of the exponential term in Eq. (3.40). It is an expected result because the non-ideal boundary conditions are chosen in a secular term form. Therefore, non-ideal boundary conditions change the stability of system. New stability situations, changing with non-ideal boundary conditions, can be found from Eq. (3.37). If Z_1 term equals to zero, then the system is bounded. The system is stable in case of negative value of Z_1 , otherwise unstable.

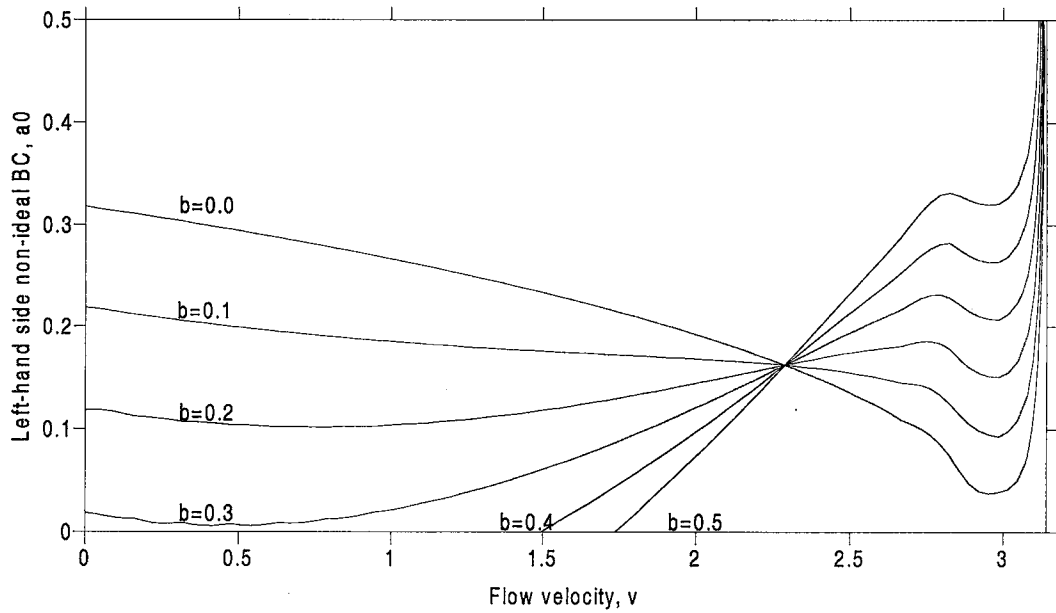


Figure 3.4 Variation of stability boundaries for constant amplitude of right-hand side for the first mode ($\beta=0.8$, $\epsilon=0.1$, $\mu=1.0$).

Decrease of the value of μ , external damping coefficient, cause to reduce the stable area. Variations of μ change the location of the mentioned point (detailed information is going to be given later).

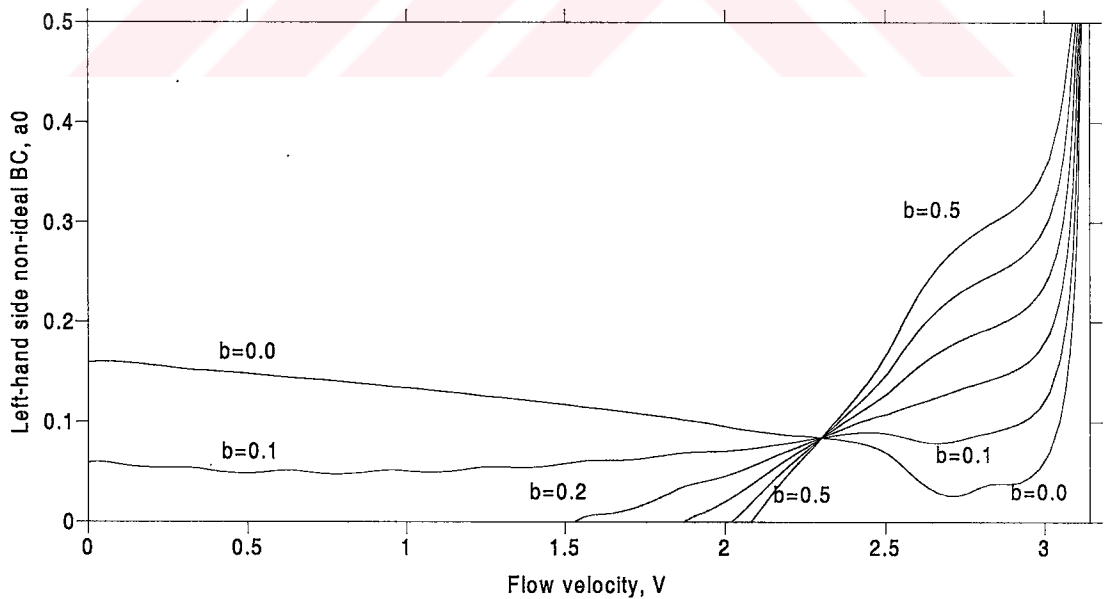


Figure 3.5 Variation of stability boundaries for constant amplitude of right-hand side for the first mode ($\beta=0.8$, $\epsilon=0.1$, $\mu=0.5$).

It doesn't change the value of flow velocity at this point. But it is acting only on along y-axis; it means the amplitude of non-ideal boundary conditions varies due to the changing value of μ .

In Figures (3.4-3.6), for first and second modes, stable and unstable regions are plotted for constant value of b_0 (amplitude of the displacement at the right support) and v (flow velocity). For constant b_0 values, stability boundaries are illustrated in Figures (3.4)-(3.6) (The b_0 values are demonstrated with the letter "b" in figures). The regions between x-axis and those lines are stable for each constant b_0 . While the value of b_0 is increasing, corresponding stable area becomes smaller in the first mode. On the contrary to the first mode, the stable area becomes larger in the second mode according to increasing b_0 value. In Figure 3.6, stable and unstable regions are shown at the second mode.

An interesting case is b_0 equal to zero. Then the system has a non-ideal boundary condition only at the left-hand side support. It means right-hand side condition is ideal. For ideal right-hand side condition, the stable boundary regions begin under the lines about $a_0=0.3$ and $a_0=0.2$ in the first mode and in the second mode, respectively. The remarkable intersection points seen from figures 3.4 and 3.5 are about $v=2.3$ and $a_0=0.17$ for the first mode and about $v=3.0$ and $a_0=0.15$ for the second mode. All stability boundary lines intersect or passed through these points. These points may have practical importance in engineering applications. If one can allow dimensionless displacement amplitude smaller than about 0.17 on one support and dimensionless flow velocity equal to 2.3, then the system is always stable at the first mode. It may be notable point for designer, who uses the boundary conditions exactly explained in this study.

Another remarkable case for designer is that the fluid velocity can be used as a controller mechanism for the system. Numerical results show that the velocities higher than the notable point allow higher amplitudes of non-ideal conditions. Then, it may be suggested that pipes can be employed in high fluid velocities for stability.

At the second mode, the location of remarkable point has small deviations from the first mode. In this case the $V \approx 3$ point defines this intersection point. A notable situation that the designer should take into account is that the regions are stable at first and second modes for the small amplitude values.

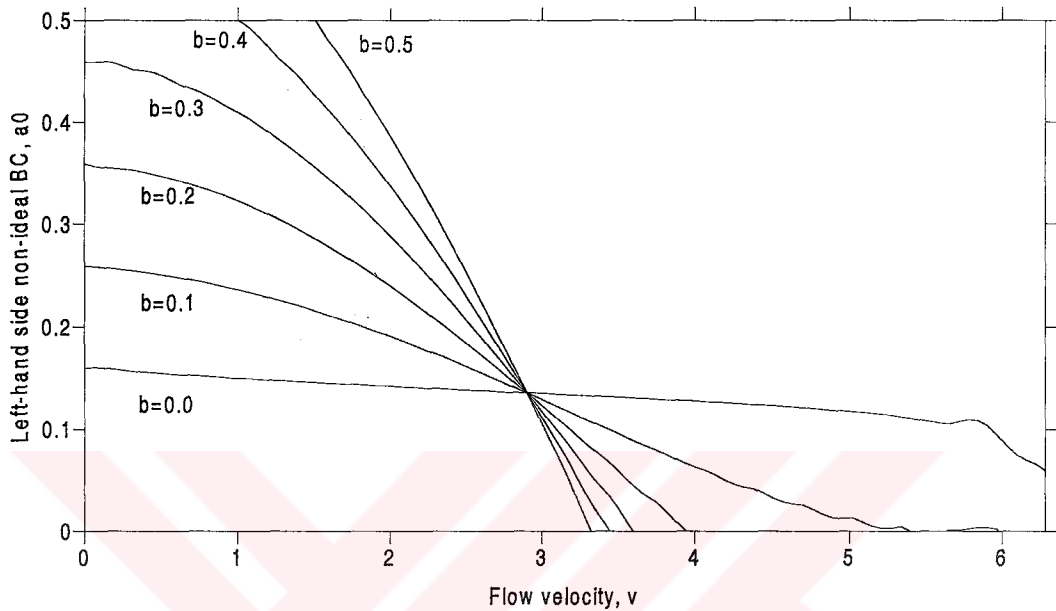


Figure 3.6 Variation of stability boundaries for constant amplitude of right-hand side for the second mode ($\beta=0.8$, $\epsilon=0.1$, $\mu=1.0$).

To see how the magnitude of non-ideal boundary conditions impose on stability conditions, the plots are drawn for different flow velocities (Figures 3.5 and 3.6). In the figures y and x axes show amplitude of non-ideal boundary conditions. The regions between y-axis and the constant flow velocity lines are considered as stable regions.

There are intersection points for the first and the second modes. The values a_0 and b_0 are equal to each other about 0.15 for the first mode (Figure 3.5) and about $a_0=0$ and $b_0=0.13$ for the second mode (Figure 3.6). With increasing flow velocity except $v=0.5$, stability boundary lines are rotating in a clock-wise direction around the point ($a_0=b_0=0.15$) for the first mode. This rotation occurs in an opposite way for the second mode around $a_0=0$ and $b_0=0.13$ in Figure (3.6).

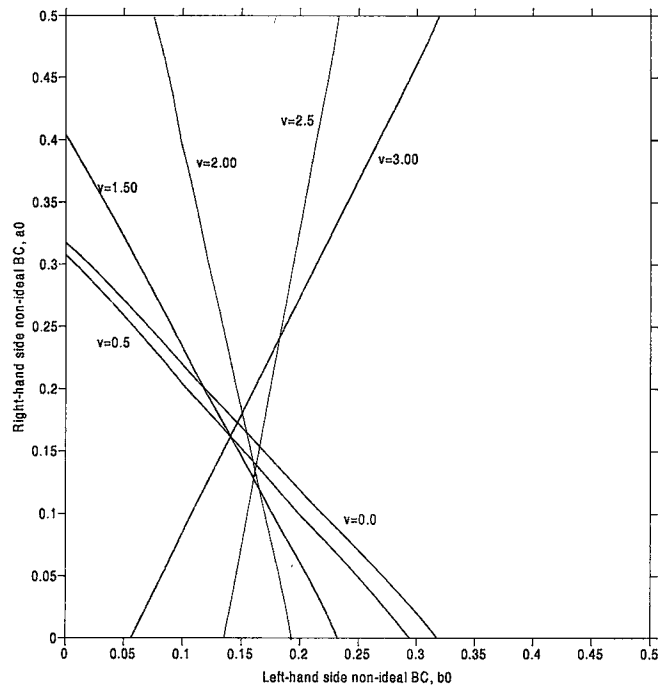


Figure 3.7 Variation of stability boundaries for constant flow velocities for the first mode ($\beta=0.8$, $\epsilon=0.1$, $\mu=1.0$).

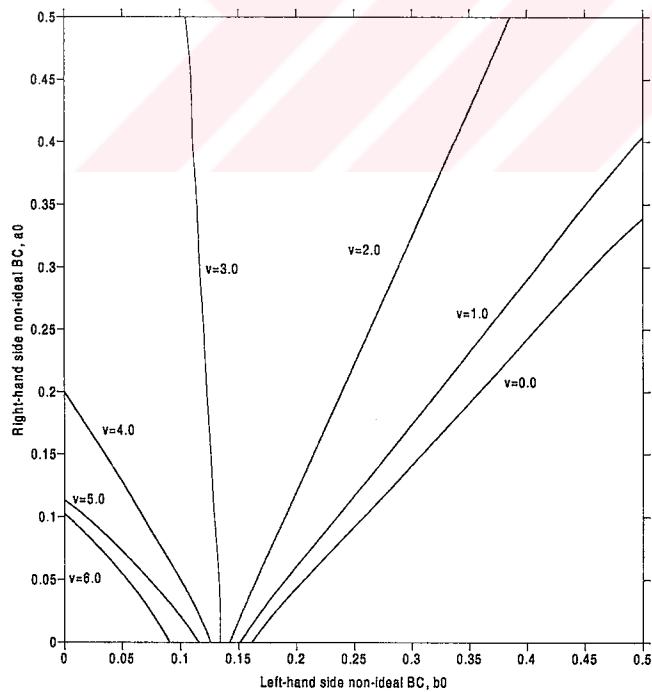


Figure 3.8 Variation of stability boundaries for constant flow velocities for the second mode ($\beta=0.8$, $\epsilon=0.1$, $\mu=1.0$).

3.3. Solution for Clamped-Clamped Pipes

Both of the boundary conditions can be accepted as non-ideal or only one is non-ideal. Now, the boundary conditions will be taken as non-ideal for both side supports. Hence, the non-ideal boundary conditions for clamped-clamped pipe are

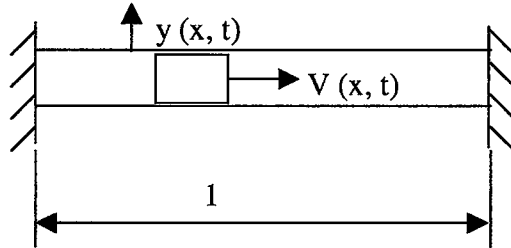


Figure 3.9 Schematics of translating continua in a pipe with clamped-clamped supports

$$y(0,t) = \varepsilon a(t), \quad y(1,t) = \varepsilon b(t) \quad (3.45a)$$

and the other conditions are

$$y'(0,t) = \varepsilon d(t), \quad y'(1,t) = \varepsilon e(t) \quad (3.45b)$$

Similar to the fixed-fixed pipe problems, variations in the displacements at the boundaries affect frequencies as well as amplitudes. The method of Multiple Time Scales is applied in search of approximate solutions. Employing the perturbation technique, separating each order, and assuming the solution is identical with fixed-fixed pipe problem in Section 3.2. Equations (3.4)-(3.10) satisfy the clamped-clamped pipe problem. The spatial function $Y_n(x)$ differs from previous problem. In spite of unchanged dispersive relation, the matrix form is changed due to the different boundary conditions (clamped-clamped), Equations 3.45a,b.

We know from previous solution that $Y_n(x)$ satisfy Equation (3.10) with below boundary conditions for clamped-clamped pipe;

$$Y_n(0)=0, Y_n(1)=0, Y'_n(0)=0, Y'_n(1)=0 \quad (3.46)$$

These boundary conditions change only the matrix. To find the matrix, the boundary conditions are applied on the spatial functions, $Y_n(x)$. Equations (3.15) and (3.17) can be used for $Y_n(0)=0$ and $Y_n(1)=0$, respectively.

from $Y'_n(0)=0$,

$$c_{1n}(i\alpha_{1n} + C_{2n}i\alpha_{2n} + C_{3n}i\alpha_{3n} + C_{4n}i\alpha_{4n}) = 0 \quad (3.47)$$

from $Y'_n(1)=0$,

$$c_{1n}(i\alpha_{1n}e^{i\alpha_{1n}} + C_{2n}i\alpha_{2n}e^{i\alpha_{2n}} + C_{3n}i\alpha_{3n}e^{i\alpha_{3n}} + C_{4n}i\alpha_{4n}e^{i\alpha_{4n}}) = 0 \quad (3.48)$$

above equations can be rewritten in matrix form,

$$\begin{bmatrix} 1 & 1 & 1 & 1 \\ i\alpha_1 & i\alpha_2 & i\alpha_3 & i\alpha_4 \\ e^{i\alpha_1} & e^{i\alpha_2} & e^{i\alpha_3} & e^{i\alpha_4} \\ i\alpha_1 e^{i\alpha_1} & i\alpha_2 e^{i\alpha_2} & i\alpha_3 e^{i\alpha_3} & i\alpha_4 e^{i\alpha_4} \end{bmatrix} \begin{Bmatrix} 1 \\ C_{2n} \\ C_{3n} \\ C_{4n} \end{Bmatrix} c_{1n} = \begin{Bmatrix} 0 \\ 0 \\ 0 \\ 0 \end{Bmatrix} \quad (3.49)$$

for non-trivial solutions, the determinant of the coefficient matrix must be zero, which yields the support condition

$$\begin{aligned} & (e^{i\alpha_{4n}} - e^{i\alpha_{3n}})(e^{i\alpha_{2n}} - e^{i\alpha_{1n}})(\alpha_{4n} - \alpha_{1n})(\alpha_{4n} - \alpha_{2n}) \\ & + (e^{i\alpha_{2n}} - e^{i\alpha_{4n}})(e^{i\alpha_{3n}} - e^{i\alpha_{1n}})(\alpha_{4n} - \alpha_{3n})(\alpha_{4n} - \alpha_{1n}) \\ & + (e^{i\alpha_{2n}} - e^{i\alpha_{3n}})(e^{i\alpha_{1n}} - e^{i\alpha_{4n}})(\alpha_{4n} - \alpha_{2n})(\alpha_{4n} - \alpha_{3n}) = 0 \end{aligned} \quad (3.50)$$

numerical values of ω_n as well as α_n can be calculated by using Equations (3.14) and (3.50).

Now, to obtain C_{2n} , C_{3n} , C_{4n} coefficients, Equation (3.15) is multiplied with α_{4n} and then subtracted from Equation (3.47)

$$c_{1n} \left[(\alpha_{4n} - \alpha_{1n}) + C_{2n} (\alpha_{4n} - \alpha_{2n}) + C_{3n} (\alpha_{4n} - \alpha_{3n}) \right] = 0 \quad (3.51)$$

in similar way, Equation (3.17) is multiplying with α_{4n}^2 and the obtained term is subtracted from Equation (3.48)

$$c_{1n} \left[(\alpha_{4n} - \alpha_{1n}) e^{i\alpha_{1n}} + C_{2n} (\alpha_{4n} - \alpha_{2n}) e^{i\alpha_{2n}} + C_{3n} (\alpha_{4n} - \alpha_{3n}) e^{i\alpha_{3n}} \right] = 0 \quad (3.52)$$

using (3.51) and (3.52), C_{2n} , C_{3n} can be obtained. Firstly Equation (3.51) is multiplied $e^{i\alpha_{3n}}$ and then Equation (3.42) is subtracted from this obtained term

$$c_{1n} \left[(\alpha_{4n} - \alpha_{1n}) (e^{i\alpha_{3n}} - e^{i\alpha_{1n}}) + C_{2n} (\alpha_{4n} - \alpha_{2n}) (e^{i\alpha_{3n}} - e^{i\alpha_{2n}}) \right] = 0 \quad (3.53)$$

C_{2n} can be driven from above equation

$$C_{2n} = - \frac{(\alpha_{4n} - \alpha_{1n}) (e^{i\alpha_{3n}} - e^{i\alpha_{1n}})}{(\alpha_{4n} - \alpha_{2n}) (e^{i\alpha_{3n}} - e^{i\alpha_{2n}})} \quad (3.54)$$

Now again same operations is applied same equations but multiplying $e^{i\alpha_{2n}}$

$$c_{1n} \left[(\alpha_{4n} - \alpha_{1n}) (e^{i\alpha_{2n}} - e^{i\alpha_{1n}}) + C_{3n} (\alpha_{4n} - \alpha_{3n}) (e^{i\alpha_{2n}} - e^{i\alpha_{3n}}) \right] = 0 \quad (3.55)$$

and then

$$C_{3n} = -\frac{(\alpha_{4n} - \alpha_{1n})(e^{i\alpha_{2n}} - e^{i\alpha_{1n}})}{(\alpha_{4n} - \alpha_{3n})(e^{i\alpha_{2n}} - e^{i\alpha_{3n}})} \quad (3.56)$$

The last coefficient, C_{4n} , is can be found using Equation (3.27)

Now those coefficients are substituting into (3.12)

$$Y_n(x) = c_{1n} \left[e^{i\alpha_{1n}x} - \frac{(\alpha_{4n} - \alpha_{1n})(e^{i\alpha_{3n}} - e^{i\alpha_{1n}})}{(\alpha_{4n} - \alpha_{2n})(e^{i\alpha_{3n}} - e^{i\alpha_{2n}})} e^{i\alpha_{2n}x} - \frac{(\alpha_{4n} - \alpha_{1n})(e^{i\alpha_{2n}} - e^{i\alpha_{1n}})}{(\alpha_{4n} - \alpha_{3n})(e^{i\alpha_{2n}} - e^{i\alpha_{3n}})} e^{i\alpha_{3n}x} \right. \\ \left. + \left(-1 + \frac{(\alpha_{4n} - \alpha_{1n})(e^{i\alpha_{3n}} - e^{i\alpha_{1n}})}{(\alpha_{4n} - \alpha_{2n})(e^{i\alpha_{3n}} - e^{i\alpha_{2n}})} + \frac{(\alpha_{4n} - \alpha_{1n})(e^{i\alpha_{2n}} - e^{i\alpha_{1n}})}{(\alpha_{4n} - \alpha_{3n})(e^{i\alpha_{2n}} - e^{i\alpha_{3n}})} \right) e^{i\alpha_{4n}x} \right] \quad (3.57)$$

The non-homogeneous problem at order ε will have a solution only if a solvability condition is satisfied. To determine this condition, steps from (3.28) to (3.36) in Section 3.2 can be followed for the clamped-clamped pipe system. Boundary conditions in Equations (3.45a and 3.45b) are

$$\begin{aligned} y_1(0, T_0, T_1) &= \psi(0, T_1) e^{i\omega_n T_0} + c.c. = a_0 A(T_1) e^{i\omega_n T_0} + c.c., \\ y_1(1, T_0, T_1) &= \psi(1, T_1) e^{i\omega_n T_0} + c.c. = b_0 A(T_1) e^{i\omega_n T_0} + c.c., \end{aligned} \quad (3.58a)$$

and

$$\begin{aligned} y_1'(0, T_0, T_1) &= \psi'(0, T_1) e^{i\omega_n T_0} + c.c. = a_1 A(T_1) e^{i\omega_n T_0} + c.c., \\ y_1'(1, T_0, T_1) &= \psi'(1, T_1) e^{i\omega_n T_0} + c.c. = b_1 A(T_1) e^{i\omega_n T_0} + c.c., \end{aligned} \quad (3.58b)$$

condition requires

$$\begin{aligned}
& -\overline{Y}_n''(1)b_0A_n(T_1)+\overline{Y}_n''(1)b_1A_n(T_1)+\overline{Y}_n''(0)a_0A_n(T_1)-\overline{Y}_n''(0)a_1A_n(T_1)= \\
& -\mu i\omega_n A_n(T_1)\int_0^1 Y_n \overline{Y}_n - 2\sqrt{\beta}VD_1A_n(T_1)\int_0^1 Y_n' \overline{Y}_n - 2i\omega_n D_1A_n(T_1)\int_0^1 Y_n \overline{Y}_n
\end{aligned} \tag{3.59}$$

Rearranging (3.59), one can write an ordinary differential equation

$$D_1A = \frac{b_0\overline{Y}_n''(1)-b_1\overline{Y}_n''(1)-a_0\overline{Y}_n''(0)+a_1\overline{Y}_n''(0)-\mu i\omega\int_0^1 Y_n \overline{Y}_n dx}{\underbrace{2\sqrt{\beta}V\int_0^1 Y_n' \overline{Y}_n dx + 2i\omega\int_0^1 Y_n \overline{Y}_n dx}_{Z=Z_1+iZ_2}} A \tag{3.60}$$

Above differential equation has a solution like (3.38) but, here, Z term is in different form. For the ideal boundary conditions, $a_{0,1} = b_{0,1} = 0$, term Z remains same as (3.39).

3.3.1 Numerical Results

The equation of motion and amplitude of vibration $A(T_1)$ term is rewritten as

$$\underbrace{\frac{\partial^4 y}{\partial x^4}}_{(i)} + V^2 \underbrace{\frac{\partial^2 y}{\partial x^2}}_{(ii)} + 2\sqrt{\beta}V \underbrace{\frac{\partial^2 y}{\partial x \partial t}}_{(iii)} + \epsilon\mu \underbrace{\frac{\partial y}{\partial t}}_{(iv)} + \underbrace{\frac{\partial^2 y}{\partial t^2}}_{(v)} = 0$$

$$D_1A = \frac{b_0\left(\overline{Y}_n''(1)+V^2\overline{Y}_n''(1)\right)-a_0\left(\overline{Y}_n''(0)+V^2\overline{Y}_n''(0)\right)-\mu i\omega\int_0^1 Y_n \overline{Y}_n dx}{\underbrace{2\sqrt{\beta}V\int_0^1 Y_n' \overline{Y}_n dx + 2i\omega\int_0^1 Y_n \overline{Y}_n dx}_{Z=Z_1+iZ_2}} A$$

Some parameters are present in these equations. Numerical results of equation of motion depend on parameters V , a_0 , b_0 , β , μ . In this section numerical results are

given with respect to V , a_0 , b_0 in graphics form. Therefore, effects of these parameters on numerical results will be seen in below figures.

Square root of β parameter in range of 0 to 1 is in equation of motion and amplitude of vibration. Therefore, β has a small effect on numerical results. So, effect of variation of β is not illustrated in figures.

Effect of external damping coefficient on numerical results are plotted in Figures 3.12-3.13.

In Figures 3.10-3.11, y-axis represents the natural circular frequency of the vibration. It is customarily measured in radians per unit time. The natural frequency, ω , has varied through 2π radians. Hence, one can write

$$\tau = \text{Period of vibration} = 2\pi/\omega$$

The natural frequency, which is the reciprocal, is defined as

$$f = \frac{1}{\tau} = \frac{\omega}{2\pi} \text{ (hz)}$$

Where, time is in dimensionless form. To compute time in dimensional form Equation (2.11) can be used.

$$y = y^* / L, x = x^* / L, t = t^* \sqrt{EI / mL^4} \quad (2.11)$$

In figures, x-axis reflects non-dimensional flow velocity, V . Non-dimensional form of velocity can be obtained from the equation below. Also, if the non-dimensional velocity (V) is known and then its dimensional form can be calculated using the equation;

$$V = vL\sqrt{\rho_f A_f / EI}$$

In this section, the numerical examples will be given for the vibrations of pipes conveying fluid with non-ideal boundary conditions for clamped-clamped supported ends. In clamped-clamped supported ends, non-ideal boundaries are examined by varying displacement and slope at ϵ order. In Figures (3.10-3.11), natural frequencies are plotted depending on velocity of fluid and amplitude of non-ideal boundary conditions for the first and second modes.

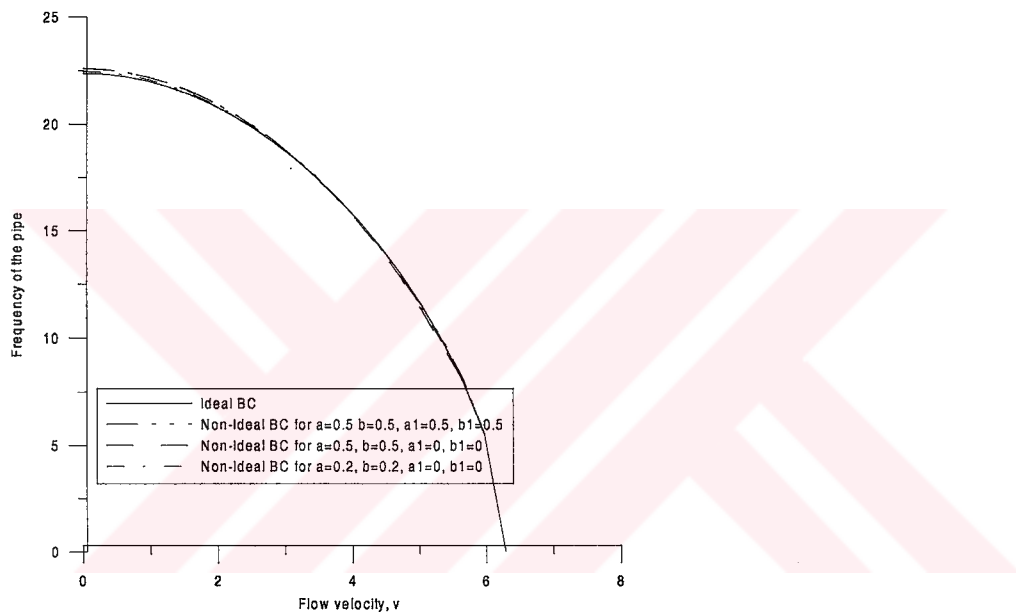


Figure 3.10 Comparisons of first natural frequencies for different non-ideal boundary conditions for clamped-clamped supports ($\beta=0.8$, $\epsilon=0.1$, $\mu=1.0$)

Depending on the mode numbers and flow velocities, the frequencies may alter in case of non-ideal boundary conditions, it may increase, decrease or remain unchanged. Increasing the velocity, the natural frequencies decrease. Varying of the ratio of fluid mass has small effect on natural frequencies due to square root of the ratio in equation of motions. At higher modes, the natural frequency values increase. The ideal and non-ideal frequencies are drawn as a function of the flow velocity.

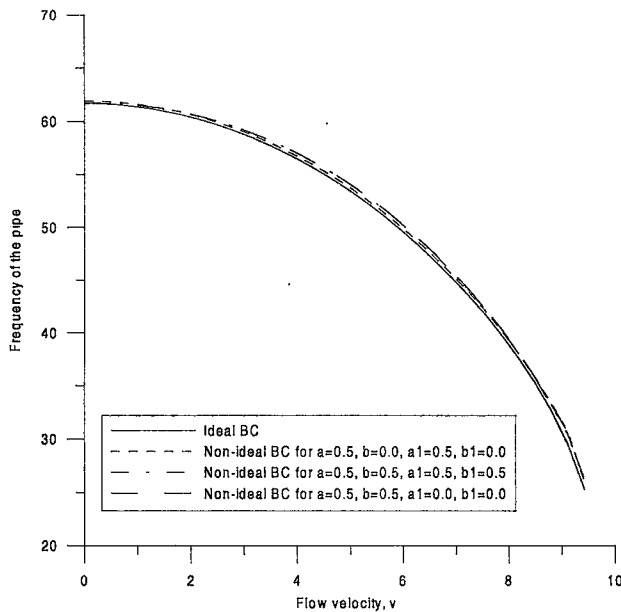


Figure 3.11 Comparisons of second natural frequencies for different non-ideal boundary conditions for clamped-clamped supports ($\beta=0.8$, $\epsilon=0.1$, $\mu=1.0$)

An interesting feature of the non-ideal boundary conditions is growth or decay of the amplitudes depending on Z argument of Eq. (3.60). It is an expected result because the non-ideal boundary conditions are chosen in a secular term form. Therefore, non-ideal boundary conditions change stability conditions. New stability conditions, changing with non-ideal boundary conditions, can be found from Eq. (3.60). If Z_1 term has a positive value, then the associated pipe is unstable.

There are two different types of non-ideal boundaries for clamped-clamped supported ends, with respect to variation displacement and slope. Both of them are in ϵ order. To show effects of the non-ideal slope on stability of pipe, three different amplitudes of the slope are considered (0.0, 0.2, 0.5). Stable and unstable regions are plotted for constant value of b_0 and v (flow velocity) for first and second modes in Figures (3.12)-(3.22). For each constant non-ideal displacement amplitude, new stability boundary is determined considering there different slope amplitudes, choosing x axis as flow velocity and y axis as amplitudes of right-hand side displacement at ϵ order in Figures (3.12-3.18). In those graphics, b_0 value is represented by letter “b”. The regions between x -axis and those lines are stable for

each constant b_0 . When the value of b_0 is increased, corresponding stable area becomes smaller. Contrary to the first mode, the stable area becomes larger in the second mode in case of increasing b_0 . To show the effect of non-ideal slopes on stability boundaries, the figures are plotted for different amplitudes of slope. The region of stability becomes smaller, when the non-ideal amplitudes of slopes increase. As before there are some remarkable intersection points. When the non-ideal amplitude of slopes increases, the points approach to x-axis. Stable and unstable regions are shown for the second mode in Figures (3.16) and (3.18).

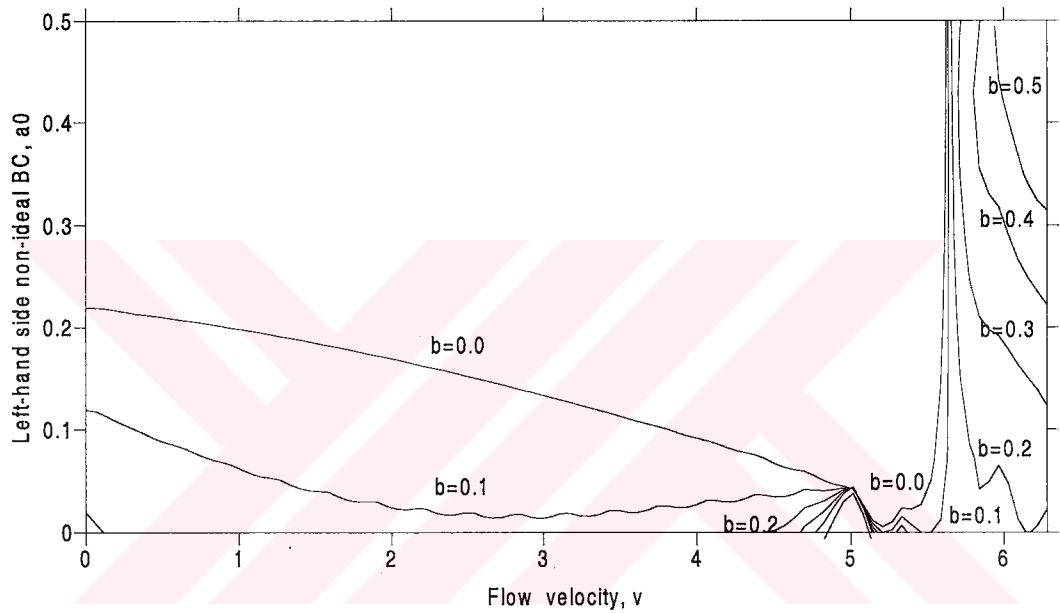


Figure 3.12 Variation of stability boundaries for constant amplitude of right-hand side for the first mode ($\beta=0.8$, $\varepsilon=0.1$, $\mu=1.0$, $a_1=0$, $b_1=0$).

Decrease of the value of μ , external damping coefficient, cause to reduce the stable area. Variations of μ change the location of the mentioned point (detailed information is going to be given later). It doesn't change the value of flow velocity at this point. But it is acting only on along y-axis; it means the amplitude of non-ideal boundary conditions varies due to the changing value of μ .

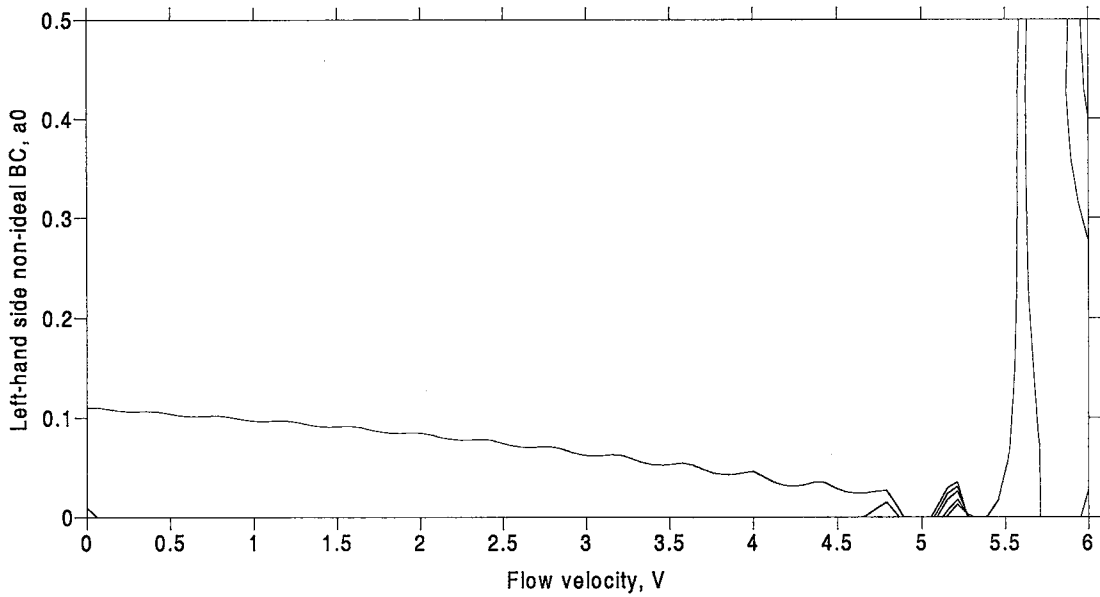


Figure 3.13 Variation of stability boundaries for constant amplitude of right-hand side for the first mode ($\beta=0.8$, $\varepsilon=0.1$, $\mu=0.5$, $a_1=0$, $b_1=0$).

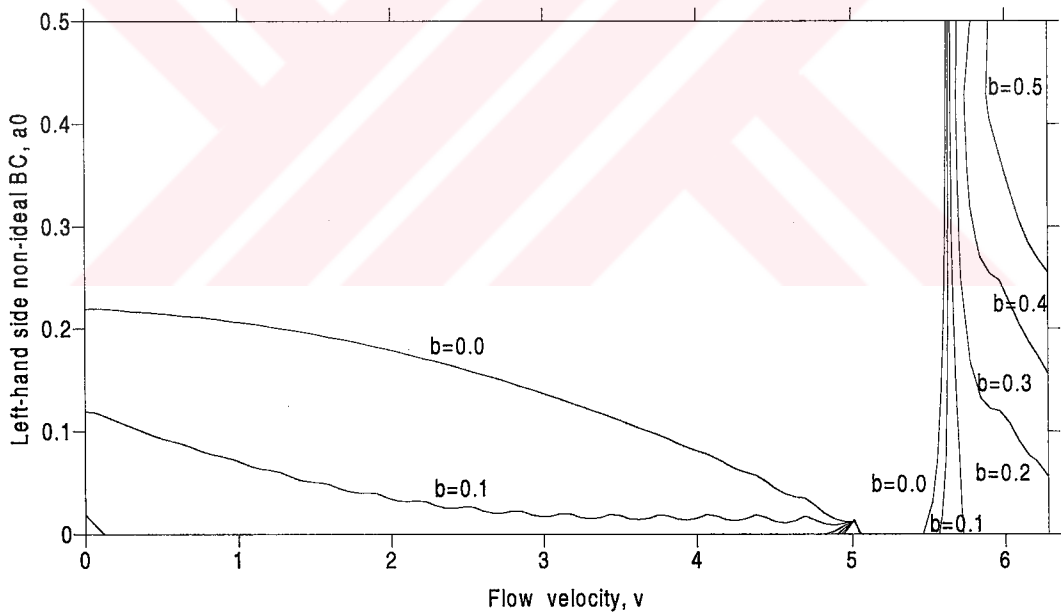


Figure 3.14 Variation of stability boundaries for constant amplitude of right-hand side for the first mode ($\beta=0.8$, $\varepsilon=0.1$, $\mu=1.0$, $a_1=0.2$, $b_1=0.2$).

An interesting case is $b_{0,1}$ equal to zero. Then the system has a non-ideal boundary condition only at the left-hand side support. It means right-hand side condition is ideal. The remarkable intersection points are seen from figures (3.12)-(3.16), for

example, $a_0 \approx 0.02$ and $V=5.0$ in Figure (3.12). All stability boundary lines intersect or passed through these points. These points may have practical importance in engineering applications. If one can allow dimensionless displacement amplitude smaller than about 0.02 on one support and dimensionless flow velocity equal to 5.0, then the system is always stable at the first mode. It may be notable point for designer, who uses the boundary conditions exactly explained in this study.

Another remarkable case for designer is that the fluid velocity can be used as a controller mechanism for the system. Numerical results show that the velocities higher than the notable point allow higher amplitudes of non-ideal conditions. Then, it may be suggested that pipes can be employed in high fluid velocities for stability.

At the second mode, the location of remarkable point has small deviations from the first mode. In this case the $V \approx 5.2$ point defines this intersection point. A notable situation that the designer should take into account is that the regions are stable at first and second modes for the small amplitude values.

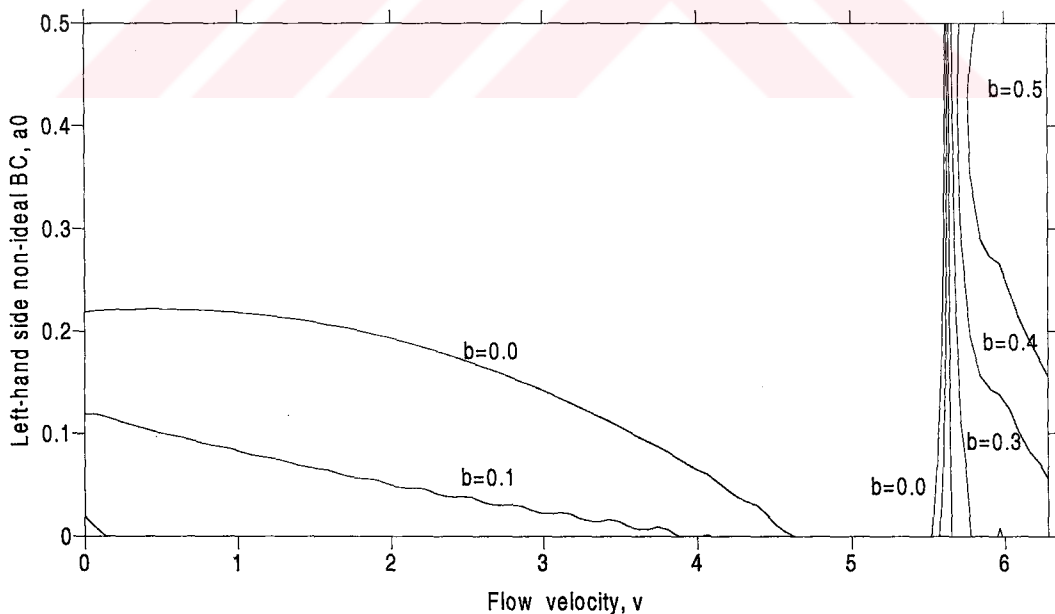


Figure 3.15 Variation of stability boundaries for constant amplitude of right-hand side for the first mode ($\beta=0.8$, $\varepsilon=0.1$, $\mu=1.0$, $a_1=0.5$, $b_1=0.5$).

At the second mode, the remarkable point location has small deviations from the first mode at V , flow velocity axis. Here, the $V \approx 5.3$ point defines remarkable point. A notable situation for designer is that for so small left-hand side amplitudes, regions are stable at first and second modes. A notable situation for designer is that for so small left-hand side amplitudes, regions are stable at first and second modes. Therefore, stability boundary line for $b_0=0$ at second mode has a specific importance. The all cases under the line are stable.

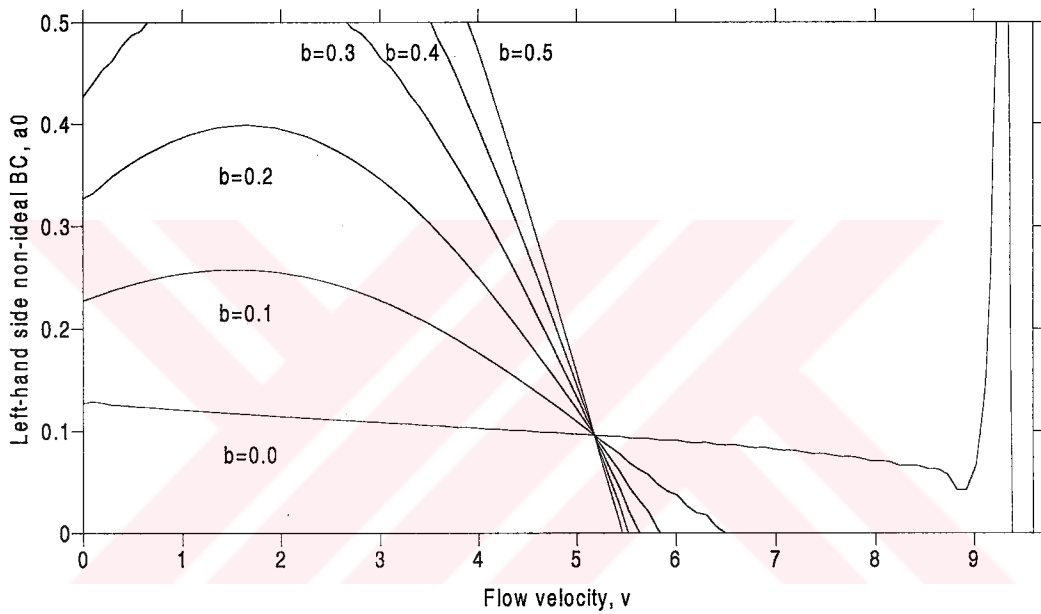


Figure 3.16 Variation of stability boundaries for constant amplitude of right-hand side for the second mode ($\beta=0.8$, $\epsilon=0.1$, $\mu=1.0$, $a_1=0.0$, $b_1=0.0$).

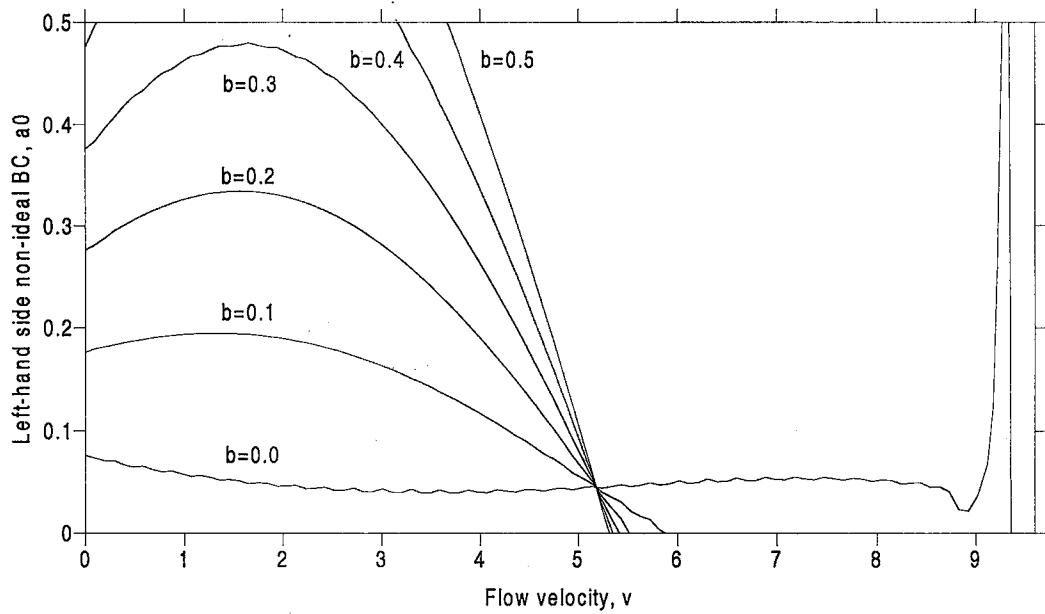


Figure 3.17 Variation of stability boundaries for constant amplitude of right-hand side for the second mode ($\beta=0.8$, $\epsilon=0.1$, $\mu=1.0$, $a_1=0.2$, $b_1=0.2$).

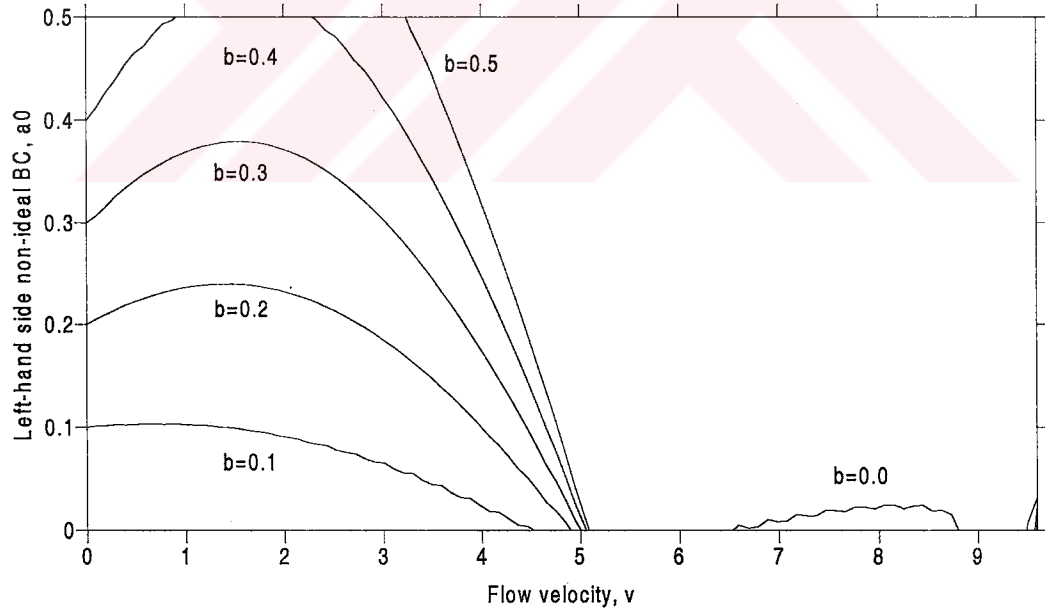


Figure 3.18 Variation of stability boundaries for constant amplitude of right-hand side for the second mode ($\beta=0.8$, $\epsilon=0.1$, $\mu=1.0$, $a_1=0.5$, $b_1=0.5$).

To see how the magnitude of amplitude of non-ideal boundary conditions impose on stability conditions, the plots are drawn for different flow shown below figures. In the figures y and x axes show amplitude of non-ideal boundary conditions. The regions between y-axis and the constant flow velocity lines are stable.

There are intersection points for the first and the second modes. The points on x-axis close to y-axis with increasing amplitude of non-ideal slopes. The values b_0 are equal to about 0.15 for the first mode (Figure (3.19)) and about $a_0=0$. and $b_0=0.1$ without non-ideal slope for the second mode (Figure 3.20)). With increasing flow velocity, stability boundary lines are rotating in a clock-wise direction around the point $(a_0=0.15, b_0=0.0)$ for the first mode. Variation on amplitude of non-ideal slope has no effect on stability lines for $v=0.0$ at the first mode. This rotation occurs in an opposite way for the second mode around $a_0=0$. and $b_0=0.1$ for no non-ideal slope in Figure (3.20).

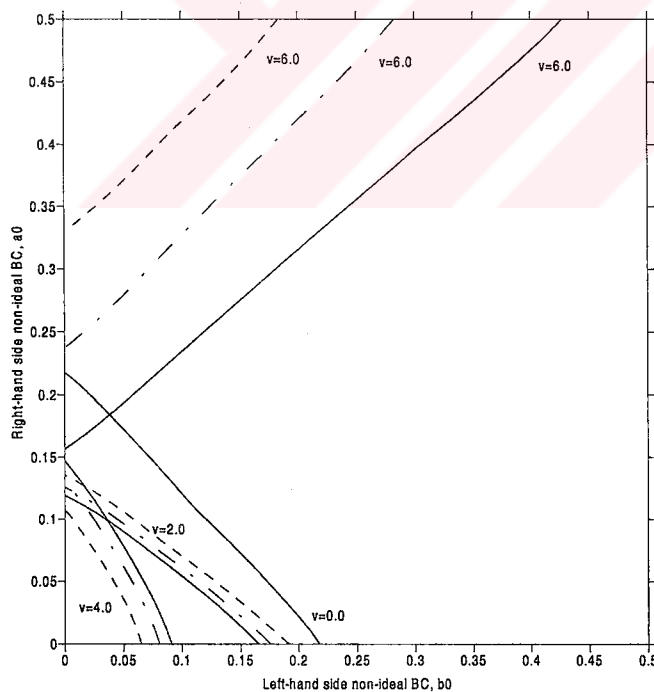


Figure 3.19 Variation of stability boundaries for constant flow velocities for the first mode ($\beta=0.8$; $\epsilon=0.1$; (—) $a=0.0, b=0.0$; (---) $a=0.2, b=0.2$; (- - -) $a=0.5, b=0.5, \mu=1.0$).

In Figures (3.19-3.22) y and x axes show the amplitude of non-ideal displacement boundary conditions. Stability boundary lines are drawn for constant flow velocity. Regions between y-axis and the lines are considered as stable regions. To show effect of non-ideal slope, lines, which have different amplitudes of non-ideal slopes, in different forms are drawn in Figure (3.19) for the first mode.

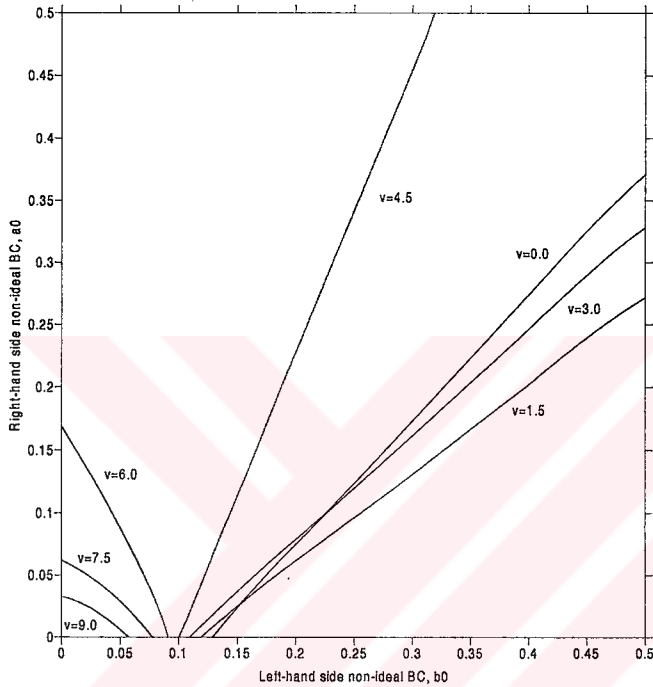


Figure 3.20 Variation of stability boundaries for constant flow velocities for the second mode ($\beta=0.8$, $\epsilon=0.1$, $\mu=1.0$, $a_1=0.0$ $b_1=0.0$)

For the second mode, effect of magnitude of non-ideal slopes is illustrated in Figures (3.20-3.22). With increasing flow velocity, the stable regions become smaller except $v=6.0$ for the first mode.

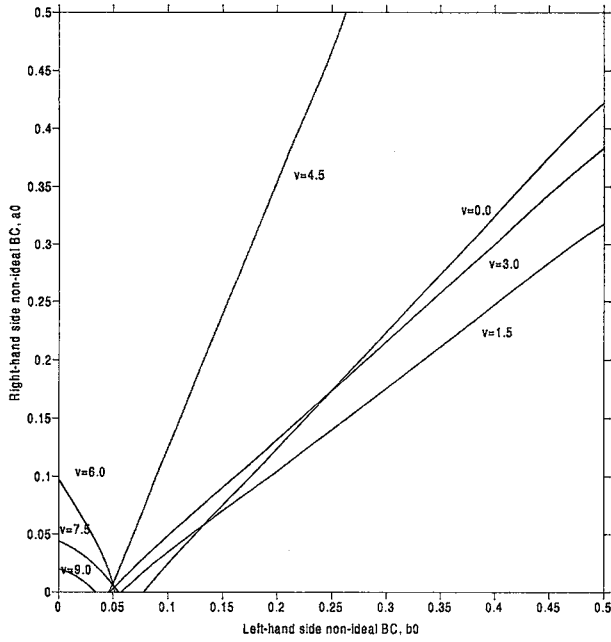


Figure 3.21 Variation of stability boundaries for constant flow velocities for the second mode ($\beta=0.8, \epsilon=0.1, \mu=1.0, a_1=0.2, b_1=0.2$)

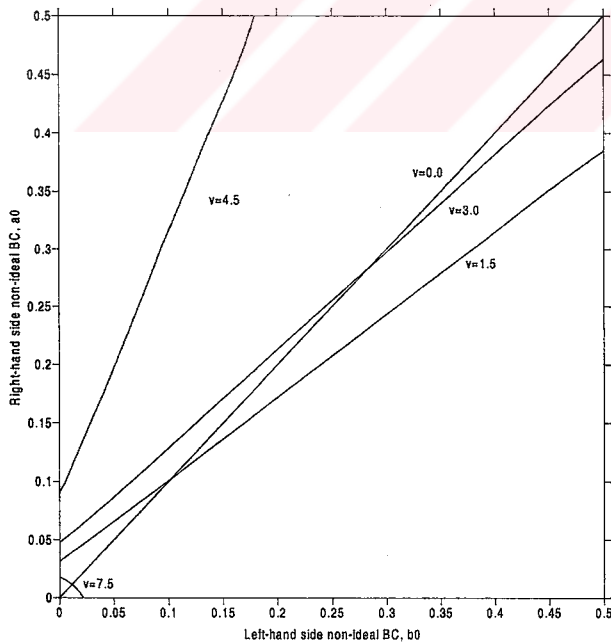


Figure 3.22 Variation of stability boundaries for constant flow velocities for the second mode ($\beta=0.8, \epsilon=0.1, \mu=1.0, a_1=0.5, b_1=0.5$)

CHAPTER FOUR

FINITE DIFFERENCE SOLUTION OF THE
EQUATION OF MOTIONS

4.1 Finite Difference Solution of the Equation of Motions.

One rewrites the equation of motion of pipes conveying fluid at constant velocity in non-dimensional form,

$$\frac{\partial^4 y}{\partial x^4} + V^2 \frac{\partial^2 y}{\partial x^2} + 2\sqrt{\beta V} \frac{\partial^2 y}{\partial x \partial t} + D \frac{\partial y}{\partial t} + \frac{\partial^2 y}{\partial t^2} = 0 \quad (4.1)$$

Boundary conditions to complement the equation of motion for simply supported pipe are

$$\begin{aligned} y(0,t) &= a(t), & y(1,t) &= b(t), \\ y''(0,t) &= y''(1,t) = 0 \end{aligned} \quad (4.2)$$

One can also write boundary conditions for clamped-clamped pipe

$$\begin{aligned} y(0,t) &= a(t), & y(1,t) &= b(t), \\ y'(0,t) &= d(t), & y'(1,t) &= e(t) \end{aligned} \quad (4.3)$$

We assume the non-homogeneous boundary conditions are changing with $e^{\sigma t} \cos \Omega t$, than Eq.(4.2) and Eq.(4.3) become

for fixed-fixed pipes

$$\begin{aligned} y(0,t) &= a_0 e^{\sigma t} \cos \Omega t, & y(1,t) &= b_0 e^{\sigma t} \cos \Omega t, \\ y''(0,t) &= y''(1,t) = 0 \end{aligned} \quad (4.4)$$

for clamped-clamped pipes

$$\begin{aligned} y(0,t) &= a_0 e^{\sigma t} \cos \Omega t, & y(1,t) &= b_0 e^{\sigma t} \cos \Omega t, \\ y'(0,t) &= a_1 e^{\sigma t} \cos \Omega t & y'(1,t) &= b_1 e^{\sigma t} \cos \Omega t \end{aligned} \quad (4.5)$$

As it can be seen in above equations, there are non-homogeneous boundary conditions. Those boundary conditions, depending on the time, occur due to some events such as, installation difficulties, non-ideal manufacturing, human failure etc. Those events can be seen sharply on marine pipeline because of installation and working area conditions on seabed.

Here, a finite difference method is applied directly to the equation (4.1), (4.4) and (4.5). Terms in the equation of motion involving only the time or spatial derivatives with even order are approximated with central difference

$$\begin{aligned} \left(\frac{\partial^4 y}{\partial x^4} \right)_n^i &= \frac{y_{n+2}^i - 4y_{n+1}^i + 6y_n^i - 4y_{n-1}^i + y_{n-2}^i}{\Delta x^4}, \\ \left(\frac{\partial^2 y}{\partial x^2} \right)_n^i &= \frac{y_{n+1}^i - 2y_n^i + y_{n-1}^i}{\Delta x^2}, & \left(\frac{\partial^2 y}{\partial t^2} \right)_n^i &= \frac{y_n^{i+1} - 2y_n^i + y_n^{i-1}}{\Delta t^2} \end{aligned} \quad (4.6)$$

for simplicity, backward difference with respect to time is used of the others.

$$\left(\frac{\partial y}{\partial t}\right)_n^i = \frac{y_n^i - y_n^{i-1}}{\Delta t^2}, \quad \left(\frac{\partial^2 y}{\partial x \partial t}\right)_n^i = \frac{(y_{n+1}^i - y_{n-1}^i) - (y_{n+1}^{i-1} - y_{n-1}^{i-1})}{2\Delta x \Delta t} \quad (4.7)$$

A subscript indicates spatial node and a superscript indicates time step in the discretized forms. Substituting those finite difference schemes into equation (4.4) yields the discretized equation at the i th time and n th spatial node as

$$\begin{aligned} y_n^i = & 2y_n^i - y_n^{i-1} - (\Delta t / \Delta x^2)^2 (y_{n+2}^i - 4y_{n+1}^i + 6y_n^i - 4y_{n-1}^i + y_{n-2}^i) \\ & - V^2 (\Delta t / \Delta x)^2 (y_{n+1}^i - 2y_n^i + y_{n-1}^i) - D\Delta t (y_n^i - y_n^{i-1}) \\ & - \sqrt{\beta V} (\Delta t / \Delta x) (y_{n+1}^i - y_{n-1}^i - y_{n+1}^{i-1} + y_{n-1}^{i-1}) \end{aligned} \quad (4.8)$$

In addition, the discretized boundary conditions given by Equations (4.4) and (4.5) becomes

For fixed-fixed, central difference scheme is used to calculate second order differential boundary conditions in FDM solutions

$$\begin{aligned} y_0^i &= a_0 e^{\sigma t^i} \cos \Omega t^i, & y_N^i &= b_0 e^{\sigma t^i} \cos \Omega t^i, \\ y_{-1}^i &= 2y_0^i - y_1^i = 2a_0 e^{\sigma t^i} \cos \Omega t^i - y_1^i, \\ y_{N+1}^i &= 2y_N^i - y_{N-1}^i = 2b_0 e^{\sigma t^i} \cos \Omega t^i - y_{N-1}^i \end{aligned} \quad (4.9)$$

For clamped-clamped, forward difference scheme on right-hand and backward difference scheme on left-hand side are applied for the first order differential boundary conditions

$$\begin{aligned} y_0^i &= a_0 e^{\sigma t^i} \cos \Omega t^i, & y_N^i &= b_0 e^{\sigma t^i} \cos \Omega t^i, \\ y_{-1}^i &= (a_0 - dx * a_1) e^{\sigma t^i} \cos \Omega t^i, \\ y_{N+1}^i &= (b_0 + dx * b_1) e^{\sigma t^i} \cos \Omega t^i \end{aligned} \quad (4.10)$$

where N is the total number of short segments into discretized pipe. In the calculations, $N=20$ is used. This simple explicit method is stable when $\Delta t/\Delta x^2 < 0.5$ for the simple beam equation (Ames, 1969). Due to the two additional fluid terms and backward differencing with respect to time, $\Delta t/\Delta x = 0.005$ is used during computations to ensure numerical stability.

“To initiate oscillations, an initial distributed velocity was imposed, starting from the position of rest.” (Semercigil et al.1997). The position of rest must satisfy the non-ideal boundary conditions.

4.2. Numerical Results

In this thesis, a finite difference approximation used by Semercigil etc. (1997) is employed. They gave a direct finite difference scheme to compute equations of motion of pipes conveying fluid. The finite difference scheme used in this thesis is almost same as Semercigil’s approximation; furthermore the scheme is verified with analytical results for well-known case (simple beam case). In this case, dimensionless flow velocity (V) and damping coefficient (D) are considered as zero in Equation (4.1). The analytical solutions with both ideal and non-ideal conditions are given in the paper presented by Pakdemirli&Boyacı (2002). In the paper, solution of simple beam equation with non-ideal condition is

$$y(x,t) = \sqrt{2} \sin(n\pi x) \left(A \cos(n^2\pi^2 t) + B \sin(n^2\pi^2 t) \right) \quad n=1,2,3,\dots \quad (4.11)$$

where A and B are constant. The solution for non-ideal conditions in this paper is

$$y(x,t) = \left(\sqrt{2} \sin(n\pi x) + \varepsilon \left\{ \frac{(an^2\pi^2 + b)}{2n^2\pi^2} \sinh(n\pi x) + \frac{\cos(n\pi)}{2n^2\pi^2} (an^2\pi^2 - b)x \cos(n\pi x) \right\} \right) * \left(A \cos \left(\left(n^2\pi^2 + \varepsilon \frac{\cos(n\pi)}{\sqrt{2n\pi}} (n^2\pi^2 a - b) \right) t \right) + B \sin \left(\left(n^2\pi^2 + \varepsilon \frac{\cos(n\pi)}{\sqrt{2n\pi}} (n^2\pi^2 a - b) \right) t \right) \right) \quad (4.12)$$

For simple beam equations, the finite difference scheme is

$$y_n^i = 2y_n^i - y_n^{i-1} - (\Delta t / \Delta x^2)^2 (y_{n+2}^i - 4y_{n+1}^i + 6y_n^i - 4y_{n-1}^i + y_{n-2}^i) \quad (4.13)$$

Numerical results obtained by FDM is compared with the analytically solutions to verify this finite difference equation. The figures below shows these results:

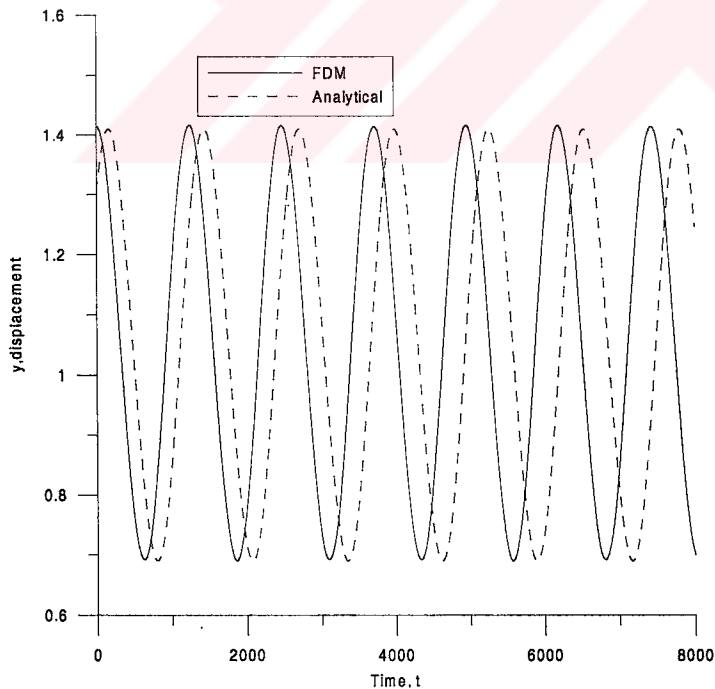


Figure 4.1. The displacement histories of fixed-fixed supports for simple beam with ideal conditions.

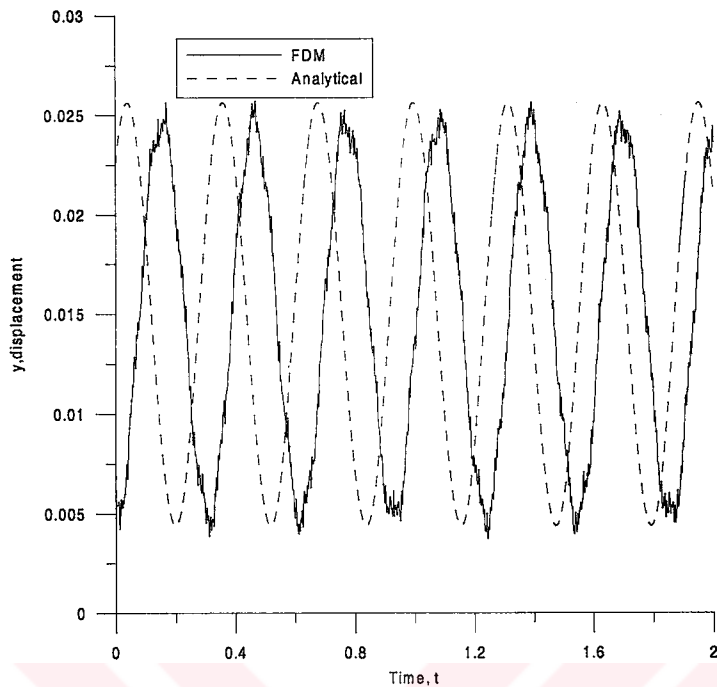


Figure 4.2. The displacement histories of fixed-fixed supports for simple beam with non-ideal conditions.

In the Figures 4.1 and 4.2, there is small difference between FDM and analytical results. Therefore one can say that this finite difference approximation shows agreement with the analytical solution.

The finite difference technique is computational solution technique but the perturbation is a semi-analytical method. The solutions found by using the perturbation method must agree with the results calculated by finite difference method (FDM). In this thesis, to show this agreement, some results obtained by perturbation technique are compared with the results calculated by FDM. The time-dependent solutions of finite differences method (FDM) are able to give displacement histories.

FDM solutions are given to show an agreement with the perturbation solutions for stable and unstable situations. The time dependent functions of non-ideal boundaries

must be known before to make computation with FDM. In multiple time scale technique, non-ideal boundary conditions are given in below form,

$$a(t) = a_0 A(\varepsilon t) e^{i\omega_n t} + c.c., \quad (4.14)$$

Expanding form $A(\varepsilon t)$ is

$$A(\varepsilon t) = C e^{Z\varepsilon t} = C e^{(Z_1 + iZ_2)\varepsilon t} \quad (4.15)$$

where C is constant and Z term can be calculated in Eq(3.37) for fixed-fixed and in Eq (3.60) for clamped-clamped. The Eq (4.14) turns into this form:

$$a(t) = a_0 e^{Z_1 \varepsilon t} e^{(\omega_n + \varepsilon Z_2) * t} + c.c. \quad (4.16)$$

where $\omega_n + Z_2$ is natural frequencies, variable depending on non-ideal boundaries and Z_1 is the real part of A term.

To make computation with FMD, natural frequencies and Z_1 must be known priory. These values are taken from the perturbation solutions and given in tables for some specific examples. Table 4.1-4.4 show some values obtained from the perturbation technique.

In this thesis two different types of support conditions are analyzed: fixed-fixed and clamped-clamped. For each type support conditions, there are two cases. The first case is the problem of pipes conveying fluid. The second case is the beam problem, which is a specific form of pipe problem. In this case flow velocity vanishes.

The values below in the tables are taken from the perturbation solutions for clamped-clamped and fixed-fixed.

Table 4.1 The values obtained by using the Multiple Time Scale for clamped-clamped supports ($a_0=b_0=0.1$, $v=5.0$, $c=0.025$, $\theta=0.0$, $\varepsilon=0.1$, $\mu=1.0$)

$a_1=b_1$	Natural frequency, Ω	Z_1 term, σ	Situation
0.00	11.603280555	0.4974974	Unstable
0.02	11.608727265	0.521611635	Unstable

Table 4.2 The values obtained by using the Multiple Time Scale for fixed-fixed supports ($a_0=0.2$, $v=2.4$, $c=0.04$, $\theta=0.0$, $\varepsilon=0.1$, $\mu=1.0$)

Non-ideal BC, b_0	Natural frequency, Ω	Z_1 term, σ	Situation
0.00	6.081953776	0.157866652	Unstable
0.05	6.066215701	0.142189064	Unstable

The values given in the Table 4.1 and 4.2 calculated with help of the Multiple Time Scale method (MTSM) are able to determine whether the system is stable or unstable. These unstable situations are also obtained by FDM using the values of columns in the tables. In the below graphics, the results obtained by using FDM and MTSM are given in a form of time histories.

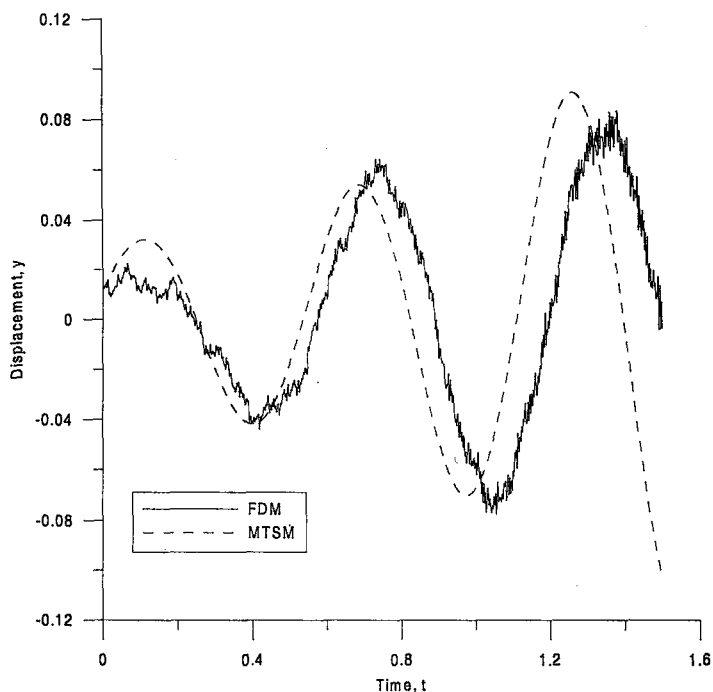


Figure 4.1. The displacement histories of clamped-clamped supports, for $a_1=b_1=0$.

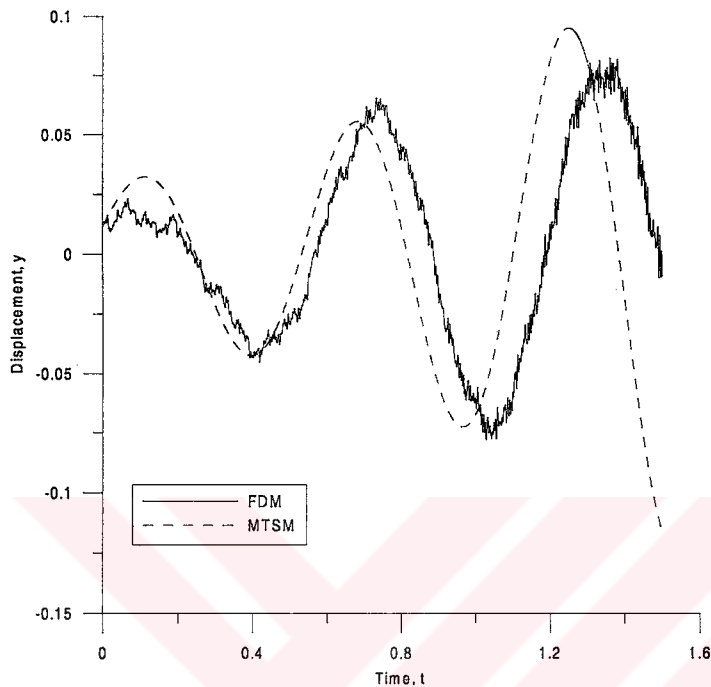


Figure 4.2. The displacement histories of clamped-clamped supports, for $a_1=b_1=0.02$.

Increasing displacement with respect to time means that the system is unstable. If the displacement is decreasing or unchanged with the time, then the system is known as stable or bounded respectively. In all Figures (4.1-4.4), the system for the pipes conveying fluid is unstable for both supports types. These results found by FDM are in agreement with the perturbation solutions. The examples in Figures (4.1-4.4), It can be seen a harmony between FDM and MTSM outcomes but there is a phase angle between them. Figures (4.4) illustrate the line obtained using FDM is fitting perfectly the line obtained using MTSM. One can see easily from the curves that the results obtained FDM agree well with the results of perturbation solutions.

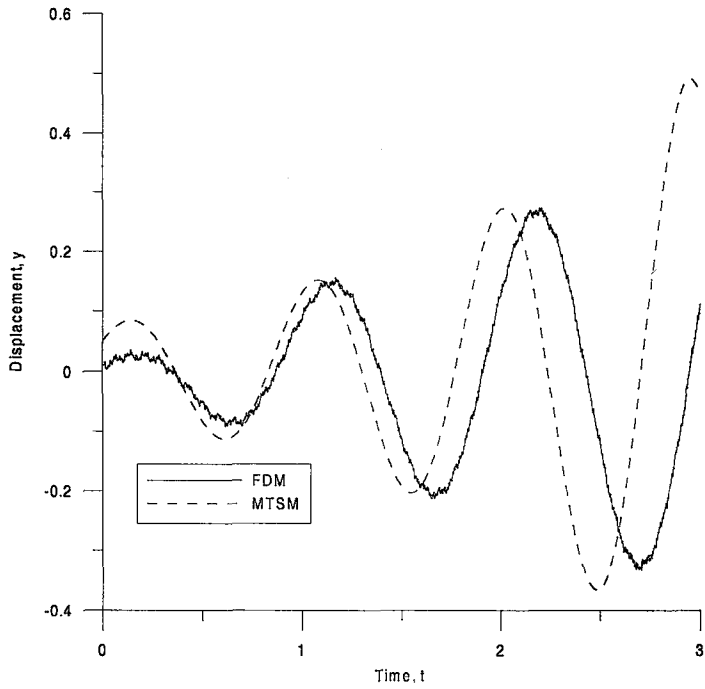


Figure 4.3. The displacement histories of fixed-fixed supports for $b_0=0.0$.

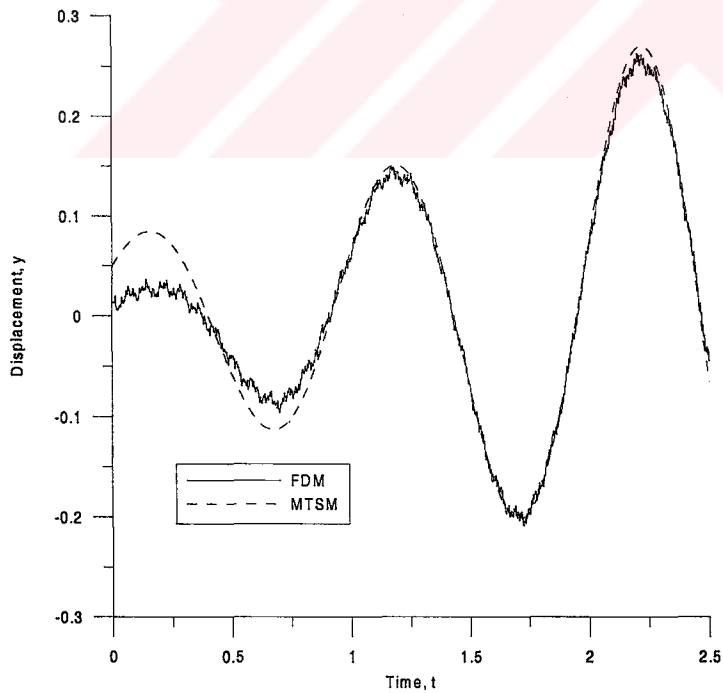


Figure 4.4. The displacement histories of fixed-fixed supports for $b_0=0.05$.

In finite difference approximation, y displacement values with regard to time are only obtained. It is called displacement histories. This graphics can be obtained just for known a fluid velocity (V), a fluid mass ratio (β) and an external damping coefficient (D). For variation of V parameter or any of them, one must recompute same finite difference scheme. And also, periods of motion are implicit form in numerical results. Spectrum analyses are required to obtain the periods. Therefore, obtaining the period of motion, displacement of the pipe with respect to time and stability conditions of the system in FDM takes too time and has too much costs. So these demanding parameters are calculated using MTSM.



CONCLUSION

Pipeline stability in critical areas of unstable and/or rapidly developing morphology is a problem of vital importance not to be unnoticed in every pipeline project. Various environmental and natural hazards with potential risks of important damage to submarine pipelines may exist along a selected pipeline route. A considerable number of pipeline damages have occurred because of unforeseen and sudden changes of the original morphology of the sea floor on which they lay.

To reduce potential risk of damage to the pipeline, the environmental threats must first be identified in the specific site, then measures be taken to protect the pipeline from these threats. The protection methods include trenching the pipeline below the seabed, anchoring of the pipeline, increased concrete coating, installation of supports installation of load/ protection mattress, gravel dumping and strengthening the pipeline. All these methods may be a kind of supports. They may have non-ideal boundary conditions.

In this study, effects of non-ideal boundary conditions on dynamic of pipes conveying fluid are investigated. The non-ideal boundary conditions are defined and formulated using perturbation theory. The results obtained by the perturbation method have agreements with the results computed with using FDM. To obtain solutions, some assumptions on non-ideal conditions have to be considered. The method of multiple time scales is applied to the equation of motion in search of approximate solutions. In solutions, two kinds of supported system are treated. Two different cases of pipe vibration problems (beam, pipe) are analyzed by using the multiple time scale and FDM.

It is shown that non-ideal boundary conditions may affect the frequencies, amplitudes of vibration as well as stability boundaries. Depending on small variation of non-ideal support conditions, amplitude of vibrations may grow or decay in time. The obtained outcomes illustrate that the fixed-fixed support conditions allow bigger amplitude of non-ideal displacement than the clamped-clamped one. The influence of small amplitude fluctuations of non-ideal boundaries on the stability of the system is investigated. The stable regions are more restricted in the case of non-ideal boundary conditions compared to the case of ideal boundary conditions.

In graphics given for constant b_0 values, there is a remarkable point. All stability boundary lines intersect or passed through this point. This point may have a practical importance in engineering applications. If one allows amplitude of displacement smaller than the amplitude at the remarkable point on one support and the value of flow velocity greater than the velocity at the remarkable point, then the system is always stable for the first mode. Hence, it could be a point for designer that they should take it into account in their engineering applications.

Another remarkable case for designer is that the fluid velocity can be used as a controller mechanism for the system. Numerical results show that the velocity higher than velocity at the mentioned point allows higher amplitude of non-ideal conditions. Then, it may be suggested that the pipes can be employed in high fluid velocity for stability. The amplitude of boundary condition on the left hand-side of the remarkable point become smaller with increasing amplitudes of slope but the corresponding fluid velocity remains unchanged.

In this thesis the velocity of flow is assumed to be constant. Similar study may be analyzed for the case the velocity varies harmonically about mean value. The equation of motions will be modified when the system has a periodic mass or existing stratified fluid in the pipe. The all pipe problems involving the ideal boundary conditions can be solved considering the non-ideal boundary conditions explained in this study.

REFERENCES

Chucheepsakul S., Monprapussorn T., Huang T. (2003) Large strain Formulations of extensible Flexible Marine Pipes Transporting Fluid. Journal of Fluids and Structures 17, 185-224.

Doare O. & De Langre E. (2002) Local and Global Instability of Fluid-Conveying Pipes on Elastic Foundations. Journal of Fluids and Structures 16(1), 1-14.

Elishakoff I. & Impollonia N. (2000) Does a Partial Elastic Foundation Increase the Flutter Velocity of a Pipe Conveying Fluid. ASME Journal Of Applied Mechanics 68 206-212.

Gaul L. & Wenzel W. (2002) A Coupled Symmetric BE-FE Method for Acoustic Fluid-Structure. Engineering Analysis with Boundary Elements 26, 629-636

Gorman D. G., Reese M. J. and Zhang Y. L. Vibration of A Flexible Pipe Conveying Viscous Pulsating Fluid Flow Journal of Sound and Vibration 230(2),379-392.

Guran A. & Atanackovic T. M. (1998) Fluid Conveying Pipe with Shear and Compressibility. Eur. J. Mech. A/Solids 17, 121-137

Impollonia N. & Elishakoff I. (2000) Effect of Elastic Foundations on Divergence and Flutter of an Articulated Pipe Conveying Fluid Journal of Fluids and Structures 14, 559-573.

- Jensen J.S. (1997) Fluid Transport Due to Nonlinear Fluid-Structure Interaction Journal of Fluids and Structures 11, 327-344.
- Kang M. G. (2000) The Influence of Rotary Inertia of Concentrated Masses on the Natural Vibrations of a Clamped-Supported Pipe Conveying Fluid Nuclear Engineering and Design 196, 281-292
- Koo G. H. & Park Y. S. (1998) Vibration Reduction by Using Periodic Supports in a Piping System. Journal of Sound and Vibration 210(1), 53-68
- Lam K. Y., Wang Q. X. and Zong Z. (2002) A Nonlinear Fluid-Structure Interaction Analysis of A Near-Bed Submarine Pipeline in A Current. Journal of Fluids and Structures 16(8), 1177-1191.
- Langthjem M. A. & Sugiyama Y. (1999) Vibration and Stability Analysis of Cantilevered Two-Pipe Systems Conveying Different Fluids. Journal of Fluids and Structures 13, 251-268.
- Lin Y.-H. & Tsai Y.-K. (1997) Nonlinear Active Vibration Control of a cantilever Pipe Conveying Fluid. Journal of Sound and Vibration 202(4), 477-490.
- Lin Y.-H. & Tsai Y.-K. (1997) Nonlinear Vibrations of Timoshenko Pipes Conveying Fluid. Int. J. Solids Structures 34, 2945-2956.
- Nayfeh, A.H. (1981) Introduction to Perturbation Techniques. New York: Wiley.
- Hansen, N.-E.O. (1982) Vibrations to Pipe Arrays in Waves. Proc.of BOSS'82, Boston, Aug., 2, 641-650.

- Öz, H.R. & Boyacı, H. (2000), Transverse Vibrations of Tensioned Pipes Conveying Fluid With Time Dependent Velocity, Journal of Sound and Vibration 236, 259-276
- Öz, H. R. & Pakdemirli, M. (1999), Vibrations of an Axially Moving Beam With Time Dependent Velocity, Journal of Sound and Vibration 227(2), 239-257.
- H. R., Pakdemirli M., Boyaci H. (1998) Non-Linear Vibrations and Stability of an Axially Moving Beam with Time-Dependent Velocity International Journal of Non-Linear Mechanics 36, 107-115.
- Öz H. R., Pakdemirli M., Özkaya E. (1998) Transition Behavior String to Beam for An Axially Accelerating Material Journal of Sound and Vibration 215(3), 571-576.
- Nedergaard, H., Hansen, N.-E.O. & Fines, S. (1982) Response of Free Hanging Tethers. Proc.of BOSS'94, Massachusetts Inst. Of Technology, July 12-15., 2, 315-326.
- Paidoussis, M.P. & Li, G.X. (1993), Pipes Conveying Fluid: a Model Dynamical Problem Journal of Fluids and Structures 7, 137-204.
- Pakdemirli M. & Boyacı H., (2001) Vibrations of a Stretched Beam with Non-ideal Boundary Conditions, Mathematical and Computational Applications 6, 217-220.
- Pakdemirli M. & Boyacı H.,(2002), Effect of Non-ideal Boundary Conditions on the vibrations of continuous system, Journal of Sound and Vibration, 249, 815-823.
- Price N. M., Liu M. et al. (1998) Vibrations of Cylindrical Pipes and Open Shells Journal of Sound and Vibration 218(3),361-387.

- Semercigil, S.E., Turan, O.F., & Lu, S. (1997), Employing Fluid Flow In A Cantilever Pipe For Vibration Control, Journal of Sound and Vibration, 205, 103-111
- Sumer, B.M. & Fredsoe, J. (1997), Hydrodynamics Around Cylindrical Structures. World Scientific Publishing
- Vendhan C. P., Bhattacharyya S. K., Sudarsan K. (1997) Stability Characteristics of Slender Flexible Cylinder in Axial Flow by the Finite Element Method Journal of Sound and Vibration 208(4),587-601.
- Wang, X. & Bloom, F. (1999) Dynamics of a Submerged and Inclined Concentric Pipe System with Internal and External Flows, Journal of Fluids and Structures 13, 443-460.
- Wu J. -S. & Shih P. -Y. (2001) The Dynamic Analysis of a Multispan Fluid-Conveying Pipe Subject to External Load Journal of Sound and Vibration 239(2), 201-215.
- Zhu F. (1995) Vibration and Stability Control of Torodial Shells Conveying Fluid Journal of Sound and Vibration 183(2),197-208.